




Cite this: *Green Chem.*, 2026, **28**, 3911

## Lignin-enabled Li-ion battery components: recent advances and outlook

Enoch Abeeku Aidoo and Pedram Fatehi \*

With the finite nature of fossil resources, rising energy demands, and the environmental impact of conventional battery materials, the shift toward bio-based materials in energy storage systems has become crucial. Lignin, the second most abundant polymer in nature and a by-product of paper & pulping and ethanol production facilities, has attracted significant research interest due to its inherent benefits, including high carbon content, renewability, robust structure, and low cost. This critical review provides a comprehensive and comparative analysis of recent advances in the incorporation of lignin into lithium-ion battery components, including anodes, cathodes, binders, separators, and electrolytes. Beyond summarizing reported electrochemical performance, this review critically examines how lignin source, structural heterogeneity, molecular weight distribution, functional group chemistry, and fractionation strategies govern structure–property–performance relationships across different battery components. Lignin-derived hard carbons have demonstrated competitive anode capacities, reaching up to 602 mAh g<sup>-1</sup> in silicon–lignin composites, while lignin-based cathode systems exploit quinone-type redox activity in hybrid architectures. In non-active components, lignin-based binders and separators offer clear advantages through aqueous processability, strong adhesion, enhanced thermal stability, and improved electrolyte affinity, whereas lignin-containing polymer and gel electrolytes exhibit ionic conductivities up to 10<sup>-3</sup> S cm<sup>-1</sup> at room temperature. Sustainability considerations, including life-cycle assessment, solvent replacement, recycling compatibility, and emerging commercialization efforts, are critically evaluated to contextualize lignin’s realistic industrial potential. Despite these advances, challenges related to intrinsic conductivity, structural variability, interfacial stability, and long-term cycling still remain unsolved. This review identifies key research directions, such as controlled fractionation, targeted functionalization, and hybrid material design, required to bridge performance gaps and enable scalable, low-carbon lithium-ion battery technologies. To achieve commercialization, the lignin-derived batteries should have 1000 stable cycles, and over 250 Wh kg<sup>-1</sup> energy density, and cost less than \$100 k<sup>-1</sup> Wh<sup>-1</sup>.

Received 28th October 2025,  
Accepted 19th January 2026

DOI: 10.1039/d5gc05761b

rsc.li/greenchem

### Green foundation

- 1 This work critically reviews the state of the art in incorporating lignin into batteries for sustainable battery fabrication. The green material, *i.e.*, lignin-derived material, is a viable pathway to replace traditional batteries.
- 2 This work discusses how incorporating lignin derivatives into battery component formulations enables the manufacture of various battery components, some of which are currently under consideration for commercialization.
- 3 In future work, the formulation can be further optimized to incorporate more lignin derivatives, resulting in improved performance for broader applications.

## Introduction

Energy storage materials are critical for harnessing, storing, and efficiently utilizing energy, particularly in applications

such as portable electronics, electric vehicles, and renewable energy systems. These materials contribute to enhanced power density, energy density, and longevity, thereby driving technological advancements and promoting sustainability.<sup>1</sup> Moreover, they play a crucial role in reducing the reliance on fossil fuels by facilitating the widespread adoption of renewable energy technologies.<sup>2</sup>

Several types of batteries are employed for energy storage, including lithium-ion batteries, sodium-ion batteries, nickel-

*Green Processes Research Center and Chemical Engineering Department, Lakehead University, 955 Oliver Road, Thunder Bay, ON P7B5E1, Canada.*  
E-mail: pfatehi@lakeheadu.ca



cadmium, nickel-metal hydride, and lead-acid batteries. Amongst these battery types, lithium-ion batteries dominate the market due to their high energy density, fast charging capabilities, and long cycle life.<sup>3</sup> However, lithium-ion batteries face challenges, such as resource scarcity and environmental footprint during mining.

Even though energy storage materials are beneficial for environmental solutions for replacing fossil-based fuels, many components of the battery are made of synthetic chemicals that are harmful to the environment during production and processing. Energy storage devices are made of inorganic and/or metal electrodes, polymeric binders usually dissolved in *N*-methylpyrrolidone (NMP) solvents, a separator, and a volatile non-aqueous electrolyte. Some of these materials are fundamentally expensive and toxic, with a negative impact on the environment.<sup>4–7</sup> For these reasons, there is a need to implement more environmentally friendly materials for more effective manufacturing processes and recyclability.<sup>8,9</sup> In this respect, it is possible to replace such materials with low-cost, environmentally friendly, and abundant materials that could provide properties and features that the energy storage system demands. Developing a sustainable fabrication process for battery manufacturing offers numerous advantages, including reduced environmental impact, lower carbon footprint, and enhanced recyclability of battery components, aligning with global green goals.<sup>10</sup>

Biobased materials, such as cellulose and lignin, have been explored as sustainable battery components.<sup>11</sup> While cellulose is abundant and mechanically robust, its limited electrochemical activity restricts its use as an active electrode material. However, its excellent film-forming ability, thermal stability, and porous structure make it highly suitable for use in separators and solid gel electrolytes. In contrast, lignin, a natural polymer rich in aromatic structures, is a promising material for many applications due to its availability, sustainability, and high carbon content.<sup>12</sup> Lignin has been explored for use in high-performance resins, adhesives, bioplastics, carbon fibres, supercapacitors, water purification systems, antimicrobial agents, biobased foams, and sustainable coatings.<sup>13–18</sup>

Lignin accounts for 15–40 wt% of wood and 5–25 wt% of nonwood species.<sup>19</sup> Over 50–70 million tons of lignin are produced annually.<sup>20</sup> Lignin contains different functional groups as well as diverse aromatic ring structures, which facilitate its chemical modification and expand its potential applications. While inherently insulating, lignin can be chemically modified or combined with conductive materials to enhance its electrochemical properties.<sup>21</sup> Its redox-active functional groups enable charge storage, and its rigid polymer network provides structural stability in electrode composites.<sup>22</sup> Additionally, lignin's tunable chemistry and ability to form porous structures facilitate ion transport, making it a viable candidate for sustainable energy solutions.<sup>23</sup>

While other biopolymers, such as cellulose, chitosan, and alginate, have shown promise in battery use due to their film-forming ability, ionic conductivity, and environmental compat-

ibility, these materials have been extensively reviewed elsewhere.<sup>24,25</sup> This paper focuses specifically on lignin due to its unique functional groups, high carbon content, aromatic structure, and widespread availability as a by-product of paper and bioethanol industries, which make lignin particularly attractive for use in electrode materials and as a sustainable alternative to synthetic battery components.

Lignin has shown potential in energy storage applications, functioning as binders, electrolytes, electrodes, and separators. Several approaches have been explored for incorporating lignin into batteries, including the direct utilization of lignin as a precursor for active material synthesis.<sup>26</sup> These methods have led to the development of lignin-based composites and nanostructures with tailored architectures,<sup>27</sup> as they showed improved mechanical stability, ionic conductivity, thermal stability during battery cycling, and metal-ion exchange.<sup>28–32</sup> Recently, the role it can play as a cathode-active material in lithium-ion batteries has garnered significant attention.<sup>33</sup> Lignin-based anodes have been extensively explored, with many studies demonstrating their feasibility and high performance. Lignin-derived carbon materials have shown excellent cycling stability and comparable capacity to commercial graphite anodes.<sup>19</sup> Some of these technologies have been commercialized (Lignode®), whilst others are approaching commercialization.<sup>34–38</sup>

The journey of Li-ion batteries began in the 1970s when scientists started exploring lithium as a potential material for energy storage. Stanley Whittingham developed the first lithium battery using titanium disulfide as a cathode and lithium metal as an anode. However, this early design faced safety issues, causing batteries to catch fire due to dendrite formation.<sup>39</sup> Breakthrough came in the 1980s when John B. Goodenough used lithium cobalt oxide (LiCoO<sub>2</sub>) as a cathode, which provided higher energy density and improved stability.<sup>40</sup> In 1990, lithium-ion batteries were commercialized. Since then, Li-ion batteries have undergone improvements in energy density, safety, and performance, making them a dominant battery technology. The demand for lithium-ion batteries has surged in recent years, driven by applications in consumer electronics and electric vehicles. However, the environmental impact of traditional lithium-ion battery components, such as cobalt oxide cathodes and graphite anodes, has sparked a search for sustainable alternatives. Lithium-ion batteries are now transitioning to a more sustainable future.<sup>7</sup> This review explores the current state of research on lignin's applications in lithium-ion batteries, focusing on the role it plays in cathodes, anodes, separators, binders, and electrolytes.

## Advantages and disadvantages of lithium-based battery

Lithium-based batteries offer many advantages over other types of batteries. As a result, they are the most used batteries in modern life. They provide the highest energy density among other commercial batteries, typically ranging from 150 to



250 Wh kg<sup>-1</sup>.<sup>39</sup> They can endure 500–2000 charge–discharge cycles compared to 300–500 discharge cycles of lead acid batteries.<sup>40</sup> They also perform well in a wide range of temperatures (–20 °C to 60 °C).<sup>41</sup> They retain charge well when not in use, leading to less energy loss over time. They are used in smartphones, torchlights, laptops, electric vehicles, and hand-held power tools.

Despite their advantages and wide-ranging applications, lithium-ion batteries have a downside. They suffer from active material degradation, especially in extreme temperature conditions, aging mechanisms, and safety concerns,<sup>42</sup> which is the greatest challenge of lithium-ion batteries. The longevity of lithium-ion batteries is affected by factors such as operating temperatures, depth of discharge, charge/discharge current rate, and periods between full charge cycles.<sup>43,44</sup>

## Components of lithium-ion battery

Lithium-ion batteries' performance and stability depend on the careful design of multiple key components, each serving a specific function in the electrochemical process. These components are essential for optimizing battery performance and exploring new materials for next-generation energy storage. The fundamental building blocks of lithium-ion batteries are electrodes (cathode and anode), electrolyte, separator, binder, and current collector. Tables 1–4 summarize the components of a lithium-ion battery and their ideal properties for efficient performance. Fig. 1 shows the working principle of a lithium-ion battery.

## Lignin and its potential: functionality and redox activity of lignin

Lignin's complex aromatic structure and rich functional group content (hydroxy, carbonyl, methoxy) have positioned it as a promising material for electrochemical energy storage. Unlike conventional fossil-based carbon precursors, lignin offers a renewable, cost-effective alternative with a high carbon yield (40–55%).<sup>45,46</sup> These structural characteristics not only allow lignin to serve as a carbon precursor for anodes and cathodes but also enable redox activity when incorporated directly into electrode composites. Recent studies have explored the use of kraft lignin, organosolv lignin, and sulfonated derivatives in lithium-ion batteries. Zhang *et al.* demonstrated that carbonized kraft lignin anodes achieved a reversible capacity of 320 mAh g<sup>-1</sup> with stable cycling over 100 cycles.<sup>33</sup> Similarly, polyaniline–lignin composites have shown improved conductivity and charge-storage behavior in supercapacitor applications due to synergistic redox interactions.<sup>12</sup> Despite its potential, lignin's heterogeneity and poor intrinsic conductivity remain a challenge, prompting further research into chemical modifications and composite engineering to enhance electrochemical performance and stability. The

**Table 1** Common electrode materials (cathode and anode) and their properties

Components	Material	Voltage vs. Li/Li <sup>+</sup> /V	Specific capacity (mAh g <sup>-1</sup> )	Thermal stability (°C)	Cycle life	Conductivity (S cm <sup>-1</sup> )	Advantages	Dis-advantages	Ref.
Cathode	Lithium cobalt oxide	3.7–4.2	140–160	150–200	300–500	10 <sup>-3</sup> –10 <sup>-2</sup>	High energy Density: 500–600 Wh kg <sup>-1</sup> Cycle life up to 5000 cycles	Cost: \$40–50 kg <sup>-1</sup> Cobalt lifespan < 500 cycles Low conductivity: <10 <sup>-9</sup> S cm <sup>-1</sup>	39
	Lithium iron Phosphate	3.2–3.5	150–165	250–300	2000–5000	10 <sup>-9</sup> –10 <sup>-10</sup>			24
	Nickel manganese Cobalt oxide	3.6–4.0	160–220	200–250	1000–2000	10 <sup>-4</sup> –10 <sup>-3</sup>	High energy Density: 600–800 Wh kg <sup>-1</sup> High Capacity: ~250 mAh g <sup>-1</sup>	Thermal runaway risk at high voltage: >60 °C at 4.2 V Lifespan: <1500 cycles Expensive: >\$45 kg <sup>-1</sup> Capacity fade: 2–3% per 100 cycles	40
	Nickel cobalt Aluminum oxide	3.6–4.2	200–250	150–200	500–1500	10 <sup>-3</sup> –10 <sup>-2</sup>			
Anode	Lithium manganese oxide	3.8–4.2	100–120	200–250	500–1000	10 <sup>-5</sup> –10 <sup>-4</sup>	Cost: \$15–20 kg <sup>-1</sup> ; fast charge capability		
	Graphite	0.1–0.2	330–370	150	>500	10 <sup>-2</sup> –10 <sup>-3</sup>	Low cost: \$10 kg <sup>-1</sup> >99% Columbic coulombic efficiency >1000 cycles	Dendrite formation risk at <0.1 V Low theoretical capacity: 372 mAh g <sup>-1</sup>	53
	Silicon	0.3–0.5	3500–4200	120	<200	10 <sup>-3</sup> –10 <sup>-5</sup>	Very high Capacity: 10× graphite theoretical (4200 mAh g <sup>-1</sup> ) Extremely long cycle life: >10 000 cycles at 10 °C	High volume expansion up to 300% severe capacity fading after 100 cycles High cost; \$30 kg <sup>-1</sup> Low energy Density: <100 Wh kg <sup>-1</sup>	54
	Lithium titanate	1.5	160–175	250	>5000	10 <sup>9</sup>	Better low-temp performance (<–20 °C), suitable for Na-ion batteries	Low initial Coulombic coulombic efficiency (60–70%) Irregular structure	
	Hard carbon	0.1–0.3	300–450	150	1000–2000	10 <sup>-4</sup> –10 <sup>-3</sup>			



**Table 2** Common electrolyte materials and their properties<sup>55</sup>

Material	Ionic conductivity (S cm <sup>-1</sup> at room temperature)	Electrochemical stability window (V)	Operating temperature (°C)	Flammability	Advantages	Disadvantages
Liquid electrolyte Lithium hexafluorophosphate in EC/DMC/EMC/DEC	10 <sup>-3</sup>	0–4.5	–20 to 60	Highly flammable	High ionic Conductivity: (10 <sup>-3</sup> S cm <sup>-1</sup> )	Prone to thermal decomposition at >60 °C
Solid polymer Electrolyte (polyethylene oxide based)	10 <sup>-5</sup> –10 <sup>-3</sup>	0–4.0	20 to 80	Low flammability	Flexible, low flammability, conductivity improves at >60 °C up to 10 <sup>-3</sup> S cm <sup>-1</sup>	Low conductivity in room temp (<10 <sup>-5</sup> S cm <sup>-1</sup> )
Ceramic electrolyte (LLZO, LAGP, NASICON)	10 <sup>-4</sup> –10 <sup>-3</sup>	0–5.0	–40 to 300	Non-flammable	Nonflammable, high thermal stability (>300 °C)	Brittle, limited flexibility
Ionic liquid Electrolyte	10 <sup>-3</sup>	0–5.5	–40 to 100	Non-flammable	Non-flammable, wide electrochemical window up to 5.5 V	Very expensive: (\$100–300 kg <sup>-1</sup> ) Compatibility issues High viscosity: (60–150 cP)

**Table 3** Common separator materials and their properties<sup>56</sup>

Materials	Thickness (μm)	Porosity %	Thermal shrinkage %	Breakdown temperature (°C)	Tensile strength (MPa)	Advantages	Disadvantages
Polyethylene	10–30	30–50	20–25	130–150	100–200	Low cost: (\$1 m <sup>-2</sup> ), commercial use in >70% LIBs	High shrinkage at >120 °C Melts at 135 °C, causing short circuit risk
Polypropylene	15–25	35–50	15–20	150–170	100–200	Mechanically robust up to 200 MPa	Low wettability with electrolyte; contact angle >90°
Ceramic-coated separator (on PE or PP)	20–40	40–60	<5	>250	150–250	High thermal stability (no melting up to 300 °C) Shrinkage <5%	Cost: 3–5× higher than uncoated PE
Glass fiber separator	20–50	50–80	<1	>300	50–100	Withstand temperatures >300 °C	Expensive: \$10–15 m <sup>-2</sup> Prone to mechanical fracture

aromatic nature of lignin provides a conjugated electron system that supports charge delocalization, facilitating electron transfer processes during electrochemical cycling.<sup>47</sup> One of the most relevant functional groups in lignin for redox applications is the quinone moiety. Quinone (C=O) groups in lignin undergo reversible two-electron, two-proton redox reactions, which are critical for faradaic energy storage mechanisms in pseudocapacitive and battery electrodes.<sup>48</sup> Oxidation treatments, such as electrochemical or chemical activation, enrich the quinone and carbonyl content in lignin, enhancing its redox activity and electron exchange capability.<sup>49,50</sup> These redox-active sites contribute directly to charge storage, particularly in composite materials, such as lignin–polyaniline or lignin–graphene systems, where synergistic interactions can lead to improved capacity and cycling stability.<sup>51</sup> This redox

functionality distinguishes lignin from other biopolymers and supports its application as an active electrochemical material, rather than only as a carbon precursor (Fig. 2).<sup>52</sup>

## Lignin-based anodes

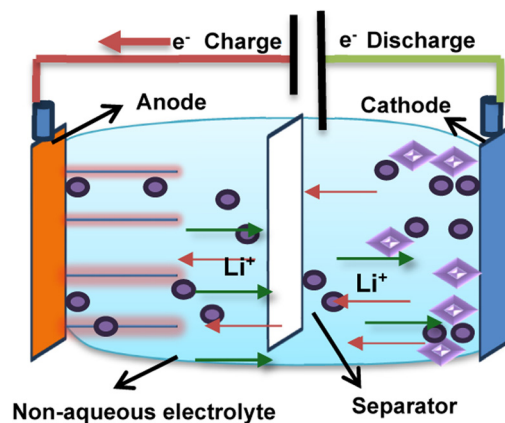
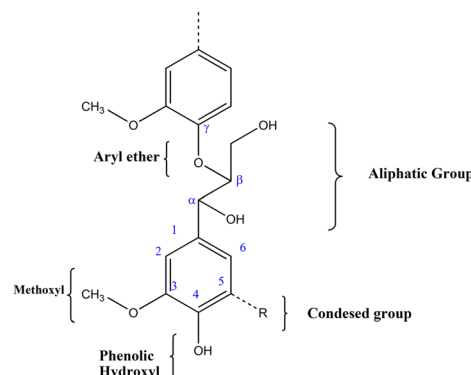
The anode is a negative electrode. It is the host of lithium ions during charging. Lithium ions move from cathodes to anodes during charging, where they are stored between layers of graphite. The ions move back to the cathode during discharge, generating an electric current.<sup>58</sup>

To ensure high performance, safety, and longevity, an ideal anode material must meet the following key requirements: (1) the anode should have a high specific capacity to store and



Table 4 Common binder materials and their properties<sup>57</sup>

Material	Solubility	Elastic modulus (m <sup>2</sup> )	Adhesion strength (N m <sup>-1</sup> )	Thermal stability (°C)	Swelling of electrolyte (%)	Advantages	Disadvantages
Polyvinylidene fluoride (PVDF)	Organic solvent	200–500	80–120	350	20	Stable up to 350 °C >95% capacity retention after 100 cycles with graphite	Moderate adhesion strength Requires toxic solvents High swelling of electrolyte (20%)
Styrene – butadiene rubber (SBR + CMC)	Water-based	50–150	200–400	300	10–15	High adhesion; >300 N m <sup>-1</sup> Water based (eco-friendly) Enables >1500 cycle life with Si/Carbon anodes	Not stable above 4.3 V Decomposes in high voltage cathodes (>4.5)
Polytetrafluoroethylene (PTFE)	Water-resistant	500–1000	100–150	>400	<5	Excellent thermal resistance (>400 °C) Low swelling in electrolytes (<5%) Strong binding properties for silicon anode	High stiffness (>500 MPa) leads to electrode cracks Difficult to process without sintering
Polyacrylic acid (PAA)	Water-based	20–100	250–400	250–300	10	Maintains 80–85% capacity after 200 cycles with silicon (Si) Can be tuned with additives	Susceptible to swelling under certain conditions Water sensitive; swelling and degradation in carbonate-based electrolytes at >10%
Polyvinyl pyrrolidone (PVP)	Water-based and polar organic solvent (ethanol, acetone, methanol)	100–300	150–250	350–400	15–20		Limited use in a commercial application Susceptible to electrolyte degradation

Fig. 1 Working principle of a lithium-ion cell. Adapted from Ghiji et al., *Energies*, 2020, 13, 5117, licensed under CC BY 4.0.Fig. 2 The main functional group in lignin's structure. Reproduced from Gonçalves et al., *Polymers*, 2021, 13, 4196, licensed under CC BY 4.0.

release lithium ions effectively. Graphite, the most widely used, has a theoretical capacity of 372 mAh g<sup>-1</sup>, while advanced materials, such as silicon, can reach 4200 mAh g<sup>-1</sup>. A high-capacity anode enhances the overall energy density of the battery, making it suitable for applications requiring long run times and power output; (2) a suitable anode must exhibit a low and stable potential relative to lithium metal to maximize the battery's operating window. The ideal anode operates close to 0.1–0.2 V vs. Li/Li<sup>+</sup>, ensuring high energy efficiency; (3) the anode must maintain its structural integrity over thousands of charge–discharge cycles. Repeated lithium insertion and extraction can cause volume expansion and contraction, leading to mechanical degradation.<sup>59</sup> Materials with high cycling stability prevent capacity fading, ensuring longer battery lifespan;<sup>60</sup> and (4) safety is paramount in lithium-ion batteries. The anode must resist thermal runaway, electrolyte decomposition, and side reactions at elevated temperatures.<sup>25</sup>

Silicon and lithium metal have been explored as anode materials, where they were aimed to increase the battery's capacity due to the materials' affinity to store more ions than

graphite.<sup>61</sup> However, challenges remain significant. High-capacity anodes, such as silicon, can undergo a volume expansion of up to 300% during cycling, leading to mechanical degradation<sup>59</sup> and swelling-induced forces in large-format cells. In addition, safety concerns, such as thermal runaway and fire hazards, continue to limit widespread adoption of lithium-ion batteries.<sup>25</sup>

The layered structure of graphite allows for reversible lithium-ion intercalation and deintercalation, enabling stable cycling.<sup>42,62,63</sup> One of the key limitations of graphite anodes is the risk of lithium plating during high-rate charging. This occurs when lithium ions are deposited as metallic lithium on the anode surface instead of intercalating into the graphite layers, which can reduce coulombic efficiency, promote dendrite formation, and increase the risk of short circuits and thermal runaway.<sup>56</sup> Due to these challenges and the environmental impact of graphite mining and purifications, there is a pressing need to explore alternatives for graphite. Biobased materials emerge as a better candidate for the next generation of lithium-ion batteries. Lignin-based anodes have been extensively explored, and the technology has been pre-commercialized as Lignode® by Stora Enso. Lignode® is a hard carbon material derived from kraft lignin, designed to replace synthetic and fossil-based graphite in lithium-ion battery anodes.<sup>38,64</sup> Key features of Lignode® include faster charge/discharge rates, improved low-temperature performance, and a reduced reliance on fossil-based graphite, when compared to conventional synthetic graphite anodes.<sup>32,64</sup> These advantages are attributed to its bio-based origin and tailored microstructure derived from kraft lignin. Its production is currently being scaled up by the Stora Enso company in Finland, with annual lignin capacity reaching 50 000 tonnes, making it a leader in this space.

Furthermore, various lignin-derived carbon composites have been investigated to improve the performance of the lithium-ion battery's anode. For example, metal-organic framework (MOF)-assisted lignin carbons improved mesopore formation and lithium-ion transport ( $6.51 \times 10^{-12} \text{ cm}^2 \text{ s}^{-1}$ ). Still, they suffered from a low carbon content and conductivity, which was later addressed through nitrogen doping.<sup>65</sup> Similarly, Culebras *et al.* developed lignin-derived carbon nanofibers (CNFs) with silicon nanoparticles that achieved excellent capacity and rate performance, though high silicon content introduced fiber uniformity issues and reduced initial coulombic efficiency.<sup>66</sup> Another research study developed lignin/PAN-derived electrospun carbon fiber (LPCF) anodes for sodium-ion batteries, with carbonization temperatures from 800–1000 °C. The LPCF-1000 sample exhibited a high specific capacity (297 mAh g<sup>-1</sup>) and excellent cycling stability (90% retention after 100 cycles), attributed to higher graphitization, optimized porosity, and improved Na<sup>+</sup> diffusion.<sup>67</sup> However, the material still showed relatively low initial coulombic efficiency (67%), primarily due to solid-electrolyte interphase (SEI) formation on its high surface area. A summary of these materials, processes, and electrochemical outcomes is presented in Table 5.

A meaningful comparison between lignin-derived hard carbon anodes and conventional synthetic graphite requires consideration of both production cost and electrochemical durability. Synthetic graphite remains the dominant commercial anode material due to its well-established manufacturing infrastructure, high electrical conductivity, and long cycle life, typically exceeding 1000–2000 cycles with capacity retention above 80% under standard operating conditions.<sup>68,69</sup> However, its production relies on energy-intensive graphitization processes (>2500 °C) and petroleum-derived precursors, resulting in high capital and environmental costs.<sup>68</sup>

In contrast, lignin-derived hard carbon benefits from low-cost, renewable feedstocks, as lignin is an abundant byproduct of the pulp and paper industry. Carbonization temperatures for lignin-based hard carbons are significantly lower (typically 800–1200 °C), leading to reduced energy consumption and lower associated CO<sub>2</sub> emissions.<sup>12</sup> Pilot-scale assessments, including those reported by Stora Enso for Lignode®, suggest that lignin-derived carbons can achieve competitive production costs when integrated into existing biorefinery infrastructure, particularly when lignin streams are valorized rather than treated as low-value waste.<sup>64</sup>

From a performance standpoint, lignin-derived hard carbons generally exhibit lower initial coulombic efficiency and shorter cycle life than synthetic graphite, primarily due to higher surface area, increased defect density, and more pronounced solid-electrolyte interphase (SEI) formation.<sup>65</sup> Typically reported cycle life for lignin-derived hard carbon anodes ranges from 300 to 800 cycles, depending on precursor quality, carbonization conditions, and electrode formulation.<sup>66,70</sup> However, these materials often demonstrate higher specific capacities than graphite and improved rate performance due to larger interlayer spacing and more accessible Li<sup>+</sup> storage sites.<sup>71</sup>

Overall, the comparison highlights a trade-off between maturity and sustainability. Synthetic graphite currently outperforms lignin-derived hard carbon in terms of long-term cycling stability, while lignin-based carbons offer advantages in feedstock renewability, energy-efficient processing, and potential cost reduction at scale. Continued advances in lignin fractionation, surface modification, and SEI stabilization are expected to narrow the performance gap, making lignin-derived hard carbons increasingly attractive for next-generation, low-carbon lithium-ion batteries.

## Lignin-incorporated cathodes

The cathode is a positive electrode and a key source of lithium ions in the battery operation. It is usually made of lithium metal oxide, such as lithium cobalt oxide, lithium manganese oxide, or lithium iron phosphate. These materials are chosen because of their affinity to release and adsorb lithium ions during charge and discharge cycles. The cathode material significantly influences the battery's energy density, voltage, and safety.<sup>39</sup> For instance, lithium cobalt oxide provides a high





Table 5 Lignin-based anodes

Active material	Preparation conditions				Specific surface area (cm <sup>2</sup> g <sup>-1</sup> )	Lithium-ion/Na-ion diffusion coefficient (cm <sup>2</sup> s <sup>-1</sup> )	Specific Capacity (mAh g <sup>-1</sup> )	Number of cycles	Retention capacity (%)	Internal resistance (Ω)	Potential range (V)	Key properties	Limitations	Solution	Ref.
	Carbonization temperature (°C)	Time (h)	Hydrothermal reaction temperature (°C)	Time (h)											
Carbonized pure lignin (CLN)					68.47	$1.14 \times 10^{-12}$	350	200	30	380	0.01–2	High surface area, abundant mesopores	Low carbon content and conductivity	Nitrogen doping to boost conductivity	65
Carbonized metal-organic framework (MOF)-based lignin (CMLN)	750	3	200	12	288.7	$6.51 \times 10^{-12}$	560	100	99	150	Vs Li/Li+				
							420	200							
							350	500							
Lignin-derived carbon nanofiber (CNF)	900		150	14	670		274	100	96.2		0.01–3	Excellent specific capacity with 15% Si content, good rate performance	Poor fiber morphology at high Si content	Optimized Si content at 10%. The capacity retention improved from 74% to 90%	66
			↓ 200	1			142	5000			Vs Li/Li+				
			↓ 250	1											
Lignin-derived carbon nanofiber/silicon (CNF/Si) 5%		0.5													
					N/A	N/A	439		94.49	N/A					
Lignin-derived carbon Nanofiber/silicon (CNF/Si) 10%								100	90.1						
							602								



Table 5 (Contd.)

Active material	Preparation conditions			Lithium-ion/Na-ion diffusion coefficient (cm <sup>2</sup> s <sup>-1</sup> )	Specific surface area (cm <sup>2</sup> g <sup>-1</sup> )	Specific Capacity (mAh g <sup>-1</sup> )	Number of cycles	Retention capacity (%)	Internal resistance (Ω)	Potential range (V)	Key properties	Limitations	Solution	Ref.
	Carbonization temperature (°C)	Time (h)	Hydrothermal reaction temperature (°C)											
Lignin-derived carbon nanofiber/silicon (CNE/Si) 15%	800	—	—	6.45 × 10 <sup>-13</sup>	257.6	921	75.4	75.4	240.1	0.01–3.0 V <sub>s</sub> Na/Na <sup>+</sup>	Low charge transfer resistance	Formation of thick solid-electrolyte interface (SEI) on high surface area carbon	Thermal optimization (carbonization at 1000 °C)	70
Lignin-PAN electrospun fiber (LPCF)	900	2	—	1.03 × 10 <sup>-12</sup>	298.9	208	100	75.6	160.6	0.01–3.0 V <sub>s</sub> Na/Na <sup>+</sup>	High surface area			
	1000	—	—	2.41 × 10 <sup>-12</sup>	356.4	267	—	89.9	98.3					

energy density but suffers from thermal instability. In contrast, lithium iron phosphate offers better safety and longer cycle life but has a lower energy density.<sup>63</sup>

An ideal cathode material for lithium-ion batteries should possess a high specific capacity, typically exceeding 150–200 mAh g<sup>-1</sup>, to store more charge per unit mass. Advanced cathode systems, such as lithium Nickel Manganese Oxide (NMC) or organic-based materials, aim for capacities in the 200–300 mAh g<sup>-1</sup> range, with emerging systems like Li-S targeting even higher values above 1000 mAh g<sup>-1</sup>.<sup>71</sup> Higher capacity implies the battery can provide more energy per charge, which is essential for applications requiring long run-times.<sup>6</sup> Higher voltage materials contribute directly to higher energy density.<sup>42</sup> Another important requirement of a cathode is high electronic and ionic conductivity to ensure an efficient electron flow and allow lithium ions to move easily within the cathode, reducing resistance and enabling fast charge/discharge. Typically, ionic conductivity values for cathode materials, such as lithium-ion phosphate (LFP), are in the range of 10<sup>-9</sup> to 10<sup>-12</sup> S cm<sup>-1</sup> at room temperature, which is relatively low and often requires conductive additives to enhance overall performance.<sup>72,73</sup>

Furthermore, the cathode material should have excellent structural stability. The cathode undergoes volume changes during lithium intercalation/deintercalation. If the structure is unstable, it can crack, leading to capacity loss and failure.<sup>42</sup> Despite their acceptable performance, the use of rare and toxic elements, for example, cobalt, increases costs and environmental impact. Thus, cathode materials should be sustainable and cost-effective.<sup>63</sup>

Traditional cathode materials, such as lithium cobalt oxide (LCO), lithium iron phosphate (LFP), and lithium nickel manganese cobalt oxide (NMC), exhibit high electrical conductivity, good theoretical capacities, and high voltage outputs. Specifically, LCO delivers a voltage of 3.9–4.2 V, LFP operates at 3.2–3.4 V, and NMC typically provides 3.6–3.8 V relative to the lithium metal/lithium-ion reference electrode (Li/Li<sup>+</sup>). Despite the promising properties, most cathode materials rely heavily on cobalt, which is expensive and environmentally damaging to mine. They also suffer from gradual capacity fading due to structural instability during repeated cycling. Recent studies have demonstrated that lignin, when functionalized or integrated into conductive composites (poly 3,4-ethylenedioxythiophene (PEDOT) or carbon nanotubes), can facilitate redox reactions *via* its quinone structures, offering reversible capacity and contributing to greener cathode alternatives. Its abundance, electrochemical activity, and tunable surface functionalities enable sustainable and low-cost cathode development without compromising performance.<sup>74</sup> For example, Navarro *et al.* developed a lignin/PEDOT hybrid *via* oxidative polymerization for lithium Li/sodium (Na)-ion batteries (reversible capacity of 80 mAh g<sup>-1</sup>, reduced polarization). However, the conductivity remained moderate and was sensitive to electrolyte anions. To address lignin's conductivity limitation, purified hydrolysis lignin was used as a cathode in primary Li batteries (with a high theoretical capacity of 400 mAh g<sup>-1</sup> at a low



Table 6 Lignin-based cathodes

Active material	Electrolyte	Application	Discharge capacity (mAh g <sup>-1</sup> )	C-rate	Number of cycles	Charge capacity (mAh g <sup>-1</sup> )	Open circuit voltage (OCV)	Capacity retention (%)	Ref.
Lignin_Conductive Carbon (C65)	1 M lithium perchlorate (LiClO <sub>4</sub> )	Lithium-ion batteries	60	C/20	25	67	2.5–3.0	N/A	75
PEDOT	1 M lithium hexafluorophosphate (LiClO <sub>4</sub> )		20			50			
	1 M lithium perchlorate (LiClO <sub>4</sub> )		44			N/A			
	1 M lithium hexafluorophosphate		50			120			
Lignin_PEDOT (20 : 80)	1 M lithium hexafluorophosphate (LiPF <sub>6</sub> )		82			92		70	
	1 M lithium perchlorate (LiClO <sub>4</sub> )		71			67		44	
Lignin_PEDOT + conductive carbon (C65)	1 M lithium perchlorate (LiClO <sub>4</sub> )		—			67		N/A	
Lignin_C65	1 M lithium hexafluorophosphate (LiPF <sub>6</sub> )		119			—		70	
	1 M lithium hexafluorophosphate (LiPF <sub>6</sub> )		60			103		N/A	
	Sodium perchlorate (NaClO <sub>4</sub> )	Sodium ion batteries	28			53			
PEDOT	Sodium hexafluorophosphate NaPF <sub>6</sub>		23			N/A			
	Sodium perchlorate (NaClO <sub>4</sub> )		34			53			
Lignin_PEDOT (20 : 80)	Sodium hexafluorophosphate		79			83		90	
	Sodium hexafluorophosphate		62			103		48	
Lignin_PEDOT + conductive carbon (C65)	Sodium perchlorate		159			—		N/A	
Hydrolysis lignin	Sodium perchlorate	Primary lithium battery	N/A	C/20	N/A	N/A	3.3	N/A	76
	1 M lithium tetrafluoroborate (LiBF <sub>4</sub> ) in $\gamma$ -butyrolactone		445	C/20		N/A			
Ligninsulfonate/polyaniline	1 M lithium perchlorate (LiClO <sub>4</sub> ) in propylene carbonate		553	1C	5000	N/A	N/A	N/A	77
	1 M Sulfuric acid (H <sub>2</sub> SO <sub>4</sub> )	Supercapacitors	254	20C		N/A		54.84	
Pure polyaniline		Supercapacitors	417	1C	5000	N/A	N/A	20.67	78
Alkaline lignin-derived phenols (LDP)	1 M sulfuric acid		416	304.5				41.88	

current density) but required conductive additives due to poor intrinsic conductivity (Table 6).<sup>75,76</sup> In another study, lignosulfonate was used as a template and dopant in *in situ* oxidative polymerization of aniline, forming a lignosulfonate/polyaniline nanocomposite with nanosphere morphology (high surface area and initial capacitance of 650 F g<sup>-1</sup>). Nevertheless, its capacity retention declined rapidly during prolonged cycling. This issue was addressed by decoupling lignin with deep eutectic solvents (DES) to form lignin-derived phenolics (LDP), which were then combined with PANI (LDP/PANI nanocomposite), achieving improved capacitance (410 F g<sup>-1</sup>), a high energy density (27.2 Wh kg<sup>-1</sup>), and excellent cycling stability over 5000 cycles (Table 6).

While each approach offers unique advantages, their suitability depends on the target application. The hybrid lignin/poly(3,4-ethylenedioxythiophene) (PEDOT) electrodes provide a promising route for rechargeable systems with balanced energy density and cycle life, despite moderate conductivity issues and sensitivity to electrolyte anions (reversible capacity ~80 mAh g<sup>-1</sup> and capacity retention >80% after 100 cycles).<sup>75</sup> The direct use of hydrolysis lignin delivers a very high theoretical capacity (400 mAh g<sup>-1</sup>) in primary lithium batteries. Still, its electrochemical performance depends strongly on the electrolyte composition, often resulting in uneven stepwise discharge profiles.<sup>76</sup> Meanwhile, lignosulfonate/polyaniline (LS/PANI) achieved a high specific capacitance (650 F g<sup>-1</sup>) and fast ion transport due to its nanosphere morphology, though capacity retention declines after extended cycling (20% loss after 1000 cycles).<sup>77</sup> These limitations were further addressed by employing lignin-derived phenolic monomers (LDP) synthesized using deep eutectic solvents (DES), which were composited with polyaniline to enhance both cycling stability (>90% after 5000 cycles) and energy density (~27.2 Wh kg<sup>-1</sup>).<sup>78</sup>

For applications requiring rechargeable and sustainable energy storage with a good compromise between capacity and long-term performance, the lignin/poly(3,4-ethylenedioxythiophene) (PEDOT) hybrid approach appears the most promising. It combines the environmental benefits of lignin with the enhanced electronic conductivity of PEDOT (10<sup>-1</sup> to 10<sup>0</sup> S cm<sup>-1</sup>), enabling improved charge transport. Electrodes based on this composite have demonstrated a reversible capacity of 80 mAh g<sup>-1</sup>, with a capacity retention >80% after 100 cycles, and coulombic efficiency >95%, making them well suited for future lithium- and sodium-ion battery technologies.<sup>75</sup>

## Lignin-based binders

A binder is a polymer material in lithium-ion batteries that binds the active material, conductive agent, and current collector to form a cohesive electrode structure. It plays a vital role in ensuring mechanical integrity and maintaining consistent electrochemical performance.<sup>79,80</sup> Conventionally, binders in lithium-ion batteries are polymeric materials (*e.g.*, PVDF, CMC, PAA), which are fabricated into solvents to prepare a slurry for electrode coating.<sup>52</sup> However, these conventional binders

present several drawbacks, such as low electronic conductivity, poor mechanical strength at high electrode loadings, and environmental concerns, particularly in the case of PVDF, which requires toxic *N*-methyl-2-pyrrolidone (NMP) as a processing solvent. These limitations have prompted research into more sustainable, conductive, and mechanically robust alternatives.

Lignin is being explored as a binder in lithium-ion batteries because, when processed into a solid polymeric film, it exhibits a high modulus elasticity (about 2–10 GPa) and the tensile strength (30–70 MPa), which are essential for maintaining electrode integrity during repeated charge and discharge cycles.<sup>14</sup> Lignin's cross-linked, highly condensed polyphenolic structure provides multiple interaction points with active material particles, promoting strong interfacial adhesion.<sup>81</sup> This rigid, three-dimensional network resists deformation under mechanical stress, helping the electrode maintain its structural integrity during repeated cycling.<sup>82</sup> Additionally, the abundant hydroxyl (–OH) groups in lignin form hydrogen bonds with both the active material and conductive additives, improving cohesion within the electrode matrix and enhancing its mechanical strength.<sup>83</sup> These characteristics make lignin a viable natural binder, capable of replacing synthetic polymers while maintaining or improving electrode durability.<sup>84</sup>

Several studies have demonstrated the potential of lignin as a sustainable binder in lithium-ion battery electrodes, with performance outcomes varying by methodology. For instance, Kraft lignin dissolved in acetone was used in both Lithium iron phosphate (LFP) cathodes and graphite anodes, showing good rate capability (117 mAh g<sup>-1</sup>) and (160 mAh g<sup>-1</sup>) at 1C for LFP cathodes and graphite anodes, respectively, and low ohmic resistance; however, dissolution in electrolyte occurred due to low molecular weight fractions of lignin.<sup>85</sup> This issue was later mitigated by pre-treating lignin with diethyl carbonate (DEC) and adding plasticizers to enhance electrolyte stability and flexibility.<sup>85</sup>

In another study, lignin was incorporated in Lithium manganese nickel oxide (LMNO) cathodes to act as a free-radical scavenger, suppressing side reactions at the cathode-electrolyte interface. The modified electrode achieved 98.2% capacity retention after 100 cycles at 0.1C, outperforming PVDF-based systems, although conductivity assessment was limited, and higher lignin content decreased performance.<sup>30</sup>

Kraft lignin used as a binder for water-based lithium manganese cobalt oxide (NMC111) cathodes showed compatibility with aqueous slurries and yielded a comparable specific capacity (147 mAh g<sup>-1</sup> at 0.1C) to PVDF-based electrodes.<sup>86</sup> Nevertheless, film cracking during drying and lithium leaching from NMC material reduced cycling performance (Table 7).

## Lignin-based membrane separators

In batteries, the separator is a porous membrane positioned between the cathode and anode to prevent direct contact and

avoid short circuits. Its primary role is to allow the selective passage of lithium ions while blocking electron flow, ensuring that electrochemical reactions occur only at the electrodes.<sup>53,56</sup>

It is typically made from polyolefin materials, such as polyethylene or polypropylene, which provide good thermal and mechanical stability.<sup>87</sup> They also retain liquid electrolyte within their pores, making appropriate pore size (typically 0.03–1 μm), porosity (35–50%), and uniform pore distribution critical for ensuring high ionic conductivity (typically 0.5–1.5 mS cm<sup>-1</sup> under liquid electrolyte saturation).<sup>56,88</sup> Although separators do not directly participate in electrochemical reactions, they play a crucial role in enabling electron flow through the external circuit.

To perform this function effectively, separators must meet several critical requirements. One of the foremost requirements for membrane separators is high thermal stability (130–160 °C). During battery operation, elevated temperatures can cause shrinkage or deformation in the separator, leading to short internal circuits and thermal runaway.<sup>89</sup> Another important requirement of a separator is its wettability. This characteristic determines the separator's affinity to absorb and uniformly distribute electrolyte. Poor wettability can result in uneven electrolyte distribution and increased internal resistance, leading to reduced ion mobility and inconsistent battery performance.<sup>90</sup>

Furthermore, mechanical strength (80–150 MPa) is vital to ensure the structural integrity of the separator throughout repeated charge and discharge cycles. During battery operation, electrode expansion and contraction place significant mechanical stress on the separator. High tensile strength and elasticity are necessary to prevent tearing or deformation.<sup>91</sup> As the battery industry shifts towards greener solutions, environmentally friendly separators have become essential to align with global sustainability goals.<sup>92</sup> Traditional polyolefin-based separators, widely used in lithium-ion batteries, face significant limitations that hinder battery performance and safety. One of the primary challenges is their poor thermal stability. Polyolefin separators have relatively low melting points (polypropylene – 150 °C, polyethylene – 130 °C), making them prone to shrinkage under elevated temperatures. This can lead to separator failure, internal short circuit, and potential thermal runaway.<sup>93</sup> Another challenge is poor wettability due to low surface energy, which results in uneven electrolyte distribution, leading to inefficient ion transport and reduced battery performance over time.<sup>90</sup>

In contrast, lignin has emerged as a promising alternative separator material. This is because its aromatic structure provides excellent thermal stability, with decomposition temperatures ranging from 250 °C to 400 °C. This makes the lignin membrane more resistant to thermal shrinkage and degradation, enhancing battery safety in high-stress environments.<sup>92</sup> In addition, the polar functional groups of lignin, such as hydroxy (–OH) and carboxy (–COOH) groups, play a critical role in improving ionic conductivity. These groups create efficient ion transport pathways and enhance electrolyte absorption, ensuring continuous lithium-ion movement during charge





Table 7 Lignin-based binders

Binder type	Slurry composition			Coating parameters					Electrochemical measurements							
	Active material	Additives	Binder conc. (%)	Solvents	Doctor Blade Gap (DBG) ( $\mu\text{m}$ )	Mass loading ( $\text{mg cm}^{-2}$ )	Drying Temp. ( $^{\circ}\text{C}$ )	Time	Porosity %	Electrode thickness ( $\mu\text{m}$ )	Specific capacity ( $\text{mAh g}^{-1}$ )	Number of cycles	C-rate	Coulombic efficiency (%)	Bulk resistance ( $\Omega$ )	Ref.
Kraft lignin	Lithium Iron Phosphate $\text{LiFePO}_4$	Super P carbon	9	Acetone	50	1.3–1.5	110	24	60	14	148	50	C/10	9	4.2	85
	Graphite		8			1.3–1.4			70	27	305	36	C/10	99.9	N/A	
Biomass-based lignin	Lithium Manganese Nickel Oxide LMNO	Carbon black	—	Water Alkaline	N/A	1.5–1.8	60	2	N/A		280 220 160 110.8	1000	C/4 C/2 1C 1C	99.5	5.4	30
Polyvinylidene fluoride (PVDF)				N-Methyl-2-pyrrolidone (NMP)			120				44.2			99	10.7	
Kraft lignin	Nickel	Carbon black	—	N-Methyl-2-pyrrolidone (NMP)	N/A	4.4	90	24	N/A	42	141	100	C/10	N/A	36.7	86
	Manganese			Water		4.5				49	154		C/10	98.2	42.8	
Kraft lignin: carboxymethyl cellulose (2 : 7)	Cobalt Oxide			Water		5.1			46	45	147		C/2	N/A	21.2	
Polyvinylidene fluoride (PVDF)				NMP		6.6			53	63	154			99.2	22.5	
PVDF : lignin (75 : 25)	(NMC111)					4.4			53	43	153			N/A	24.1	
PVDF : lignin (50 : 50)						4.8			57	50	132				25.3	

Table 8 Lignin-based membrane separators

Separator type	Solvent for electrospinning	Composition ratio	Porosity (%)	Wettability (°)	Electrolyte uptake (%)	Ionic conductivity S cm <sup>-1</sup>	Capacity (mAh g <sup>-1</sup> )	C-rate	Retention capacity (%)	Thermal shrinkage at 150 °C (%)	Time (m)	Number of cycles	Ref.
Polypropylene (PP)	N,N-Dimethylformamide (DMF)	00:10	42	66.8±1.6	47	1.09 × 10 <sup>-5</sup>	137.5	0.2C	93.1	32	5	50	29
Lignin/polyacrylonitrile (L/PAN)		00:10	21	52.3±1.5	368	6.88 × 10 <sup>-4</sup>	48	8C	93.3	0			
Lignin/polyacrylonitrile (L/PAN)		01:09	24	41.9±1.2	414	9.94 × 10 <sup>-4</sup>	154.6	0.2C	93.5				
Lignin/polyacrylonitrile (L/PAN)		03:07	66	40.1±1.1	530	1.24 × 10 <sup>-3</sup>	167.1	0.2C	95				
Lignin/polyacrylonitrile (L/PAN)		05:05	74	31.6±1.4	790	7.75 × 10 <sup>-4</sup>	150.6	0.5C	N/A				
Lignin/polyacrylonitrile (L/PAN)							131.8	1C					
							109.5	2C					
							86.9	4C					
							63.8	8C					
							N/A	N/A	N/A				
Polypropylene (celgard 2400)	Deionized Water (DI water)		60–90	47.7	121	N/A	122.6	0.5C	88.3	45	60		94
					146	EL-Gr	88.8	1C					
					108	EL-Si	47.8	2C					
						EL-LTO	7.6	5C					
Lignin/polyvinyl alcohol (PVA)		01:01		18.3	488	2.3 × 10 <sup>-2</sup>	133.3	0.5C	95.5	15			
					508	EL-Gr	117.9	1C					
					533	EL-Si	91.2	2C					
						EL-LTO	33.4	5C					
Polyimide (PI)	N,N-Dimethylformamide (DMF)	—	N/A	N/A	N/A	N/A	113	1C	91.1	N/A	30	100	66
Polyimide/lignin (PI-L)		05:01		N/A	592	1.78 × 10 <sup>-3</sup>	135		95.1	0			
Polypropylene (PP)		—		36	N/A	N/A	91		90	N/A			



and discharge cycles.<sup>92</sup> Furthermore, the rigid aromatic backbone ensures high mechanical or thermal strength, preventing tearing or deformation under mechanical or thermal stress. This structural robustness enhances the separator's dimensional stability, even under swelling or cycling conditions.<sup>92</sup>

Several studies explored lignin as a membrane separator in lithium-ion battery applications. For example, Uddin *et al.* fabricated a composite of industrial kraft lignin with polyvinyl alcohol by electrospinning in water.<sup>94</sup> The lignin composite membrane had a uniform porous structure of 60–90%, with excellent thermal shrinkage of 15% at 150 °C, superior wettability (18.3°), and electrolyte retention (533%) as reported in Table 8. The downside of this approach is that ion transport was hindered, which affected conductivity. This was because the composite membrane had a high thickness (90 μm). Also, mechanical durability under high stress was not fully explored. Another research study fabricated a composite fiber of lignin and polyacrylonitrile by electrospinning with dimethylformamide (DMF). The resulting composite membrane had a three-dimensional fibrous network structure with interconnected pores. This demonstrated excellent ionic conductivity ( $1.24 \times 10^{-3} \text{ S cm}^{-1}$ ) due to high porosity (66%), enhanced wettability (contact angle of 40°), faster electrolyte uptake (530%), and no thermal shrinkage at 150 °C. However, an increased lignin content in the composite led to the poor dispersion of lignin within the polymer matrix, due to phase separation, resulting in a less effective and mechanically weaker composite structure.<sup>29</sup>

While both approaches demonstrated enhanced performance, the lignin/polyacrylonitrile membrane stood out for its superior thermal stability and mechanical robustness. Still, the lignin/polyvinyl alcohol demonstrated good electrolyte retention and eco-friendliness.

## Lignin-based electrolytes

An electrolyte acts as a medium that allows lithium ions to move between the cathode and anode during charge and discharge cycles. It usually consists of lithium salt dissolved in a mixture of organic solvents. It is important to note that the electrolyte must be at a stable operating voltage and allow for efficient transport<sup>6,95</sup> as reported earlier in Table 2.

For electrolytes to function properly, they should have high ionic conductivity (Table 2). High ionic conductivity implies fast lithium-ion transport, which enables efficient charge and discharge cycles. Low conductivity leads to high internal resistance, reducing power output and increasing heat generation. Another important feature of a good electrolyte is a high lithium-ion transference number, ideally close to 1.<sup>96</sup> This implies that it should selectively transport lithium ions with minimal movement of other ions present in the electrolyte. Higher lithium transference number reduces electrode polarization and improves efficiency in high-power applications. Lastly, an electrolyte must form a stable solid–electrolyte inter-

phase (SEI) with the anode to prevent lithium-ion dendrite growth.<sup>97</sup> On the other hand, the electrolyte should not excessively react with cathodes, as it leads to electrolyte decomposition and capacity loss. Also, poor electrode–electrolyte compatibility leads to high resistance, lower efficiency, and faster degradation.

The electrolyte's composition is crucial for the battery's performance and safety, particularly at high temperatures. Electrolytes in the battery can be liquid, solid, or gel (Table 2). For most traditional battery electrolytes, especially lithium-ion batteries, a liquid-type electrolyte is used. They are usually lithium salts dissolved in organic solvents. The common ones are lithium hexafluorophosphate (LiPF<sub>6</sub>) and lithium perchlorate (LiClO<sub>4</sub>) dissolved in ethylene carbonate (EC) and dimethyl carbonate (DMC). Other solid polymer electrolytes include polyethylene oxide (PEO) and polymethyl methacrylate (PMMA).<sup>97</sup> Recent studies have incorporated solid polymer and gel electrolytes. It is established that the lignin suppresses lithium dendrites and active material dissolution.<sup>98,99</sup> The oxygen-containing functional groups interact with lithium ions through coordination bonds. This helps to homogenize the lithium-ion flux at the lithium surface during deposition, leading to uniform lithium-ion distribution (lithium plating), which results in less dendrite growth on electrodes.<sup>100</sup> With this advantage of lignin as well as sustainability, researchers intend to replace traditional electrolyte polymers.<sup>97,98</sup>

In one study, polyvinylpyrrolidone (PVP) was synthesized with lignin matrix to form a composite polymer membrane. The membrane was then soaked in a liquid electrolyte to form a gel polymer electrolyte (LP-GPE). The gel polymer electrolyte exhibited high ionic conductivity ( $2.52 \times 10^{-3} \text{ S cm}^{-1}$ ) at room temperature, improved lithium-ion transference number, and better mechanical strength (2.42 MPa).<sup>101</sup> Despite these improvements, the electrochemical stability of the gel polymer was slightly lower than that of pure lignin-based electrolyte due to the presence of polyvinylpyrrolidone, which eventually degrades over time.<sup>101</sup> Wang *et al.* blended lignin and poly(*N*-vinylimidazole)-*co*-poly(ethylene glycol) methyl ether methacrylate (LCP), forming a free-standing electrolyte membrane (meaning that the membrane is self-supporting and can keep its shape without needing to be coated on any substrate). This resulted in improved suppression of lithium dendrites, reducing the risk of short circuits.<sup>102</sup> It demonstrated over 10 times mechanical improvement over pure lignin membranes. The key performance metrics for each electrolyte membrane are summarized in Table 9. In brief, Approach 1 (LP-GPE) showed higher ionic conductivity ( $2.52 \times 10^{-3} \text{ S cm}^{-1}$ ) and better flexibility, whereas Approach 2 (LCP) demonstrated superior Li-ion transference number (0.63), and effective dendrite suppression. The choice between these approaches depends on the target application requirements.

Although lignin-based polymer and gel electrolytes currently exhibit ionic conductivities in the order of  $10^{-4}$ – $10^{-3} \text{ S cm}^{-1}$  at room temperature<sup>103,104</sup> (Table 9), several well-established strategies can be employed to enhance their ion-transport properties and electrochemical stability further.





Table 9 Lignin-based electrolytes

Membrane composite matrix	Active polymer content wt. %	Electrolyte	Fabrication method		Membrane thickness $\mu\text{m}$	Porosity %	Tensile strength (Mpa)	Electrolyte uptake %	Ionic conductivity ( $\text{S cm}^{-1}$ )	Lithium transference	Electro. stability	Rate Performance @0.5C (mAh $\text{g}^{-1}$ )	Ref.
			Method	Substrate									
Lignin/poly(N-vinylimidazole)/co-poly(ethylene glycol methyl ether methacrylate) (LCP)	67% Lignin 33%LCP	Lithium bis (trifluoromethanesulfonyl) imide (LiTFSI)	solution	Teflon	100	30	1.9	250	$2.6 \times 10^{-4}$	0.63	4.7	130	102
Lignin/polyvinylpyrrolidone (PVP) + KH-550 LP_GPE	78% Lignin 22%PVP	1 M Lithium Hexafluoro-Phosphate in EC/DMC/EMC (1 : 1 : 1 v/v)	casting	Sheet	120	33	2.42	273	$2.52 \times 10^{-3}$	0.56	4.6	145	101

Importantly, many of these approaches are compatible with green chemistry principles and scalable polymer processing.

One effective strategy involves reducing polymer crystallinity and increasing segmental mobility. Blending lignin with flexible polymers, such as poly (ethylene oxide), poly (vinyl pyrrolidone), or polyethylene glycol, disrupts chain packing and enhances  $\text{Li}^+$  transport through amorphous domains.<sup>103</sup> This effect is evident in lignin/PVP-based gel polymer electrolytes, which achieve the highest reported conductivity ( $2.52 \times 10^{-3} \text{ S cm}^{-1}$ ) due to increased free volume and enhanced polymer dynamics.<sup>103,105</sup>

A second approach is functional group engineering. Increasing the concentration of ion-coordinating groups, such as ether oxygens, carboxylates, or sulfonate moieties, can promote stronger  $\text{Li}^+$  solvation and facilitate hopping mechanisms.<sup>71</sup> The chemical modification of lignin through sulfonation, carboxylation, or grafting of ion-conductive side chains offers a tunable pathway to improve ionic conductivity while maintaining the renewable character of the material.<sup>12,71,104</sup>

Plasticization and gel formation represent another widely used strategy. Incorporating small-molecule plasticizers or ionic liquids into lignin-based polymer matrices enhances chain flexibility and creates continuous ion-conduction pathways. Excessive plasticizer content can compromise mechanical integrity, optimized gel polymer electrolytes, balance conductivity, mechanical strength, and electrochemical stability.<sup>104</sup>

In addition, nanostructuring and filler incorporation can improve both conductivity and stability. The introduction of ceramic nanoparticles or bio-derived fillers can suppress polymer crystallization, stabilize the electrode–electrolyte interface, and widen the electrochemical stability window by immobilizing anions and reducing interfacial side reactions.<sup>103</sup>

Finally, improving electrolyte performance requires interface-focused design. The surface modification of lignin-based electrolytes to enhance wettability and interfacial contact with electrodes can reduce interfacial resistance and mitigate lithium dendrite formation. These strategies suggest that the current conductivity values reported for lignin-based electrolytes should be viewed as an early-stage benchmark rather than a fundamental limitation.<sup>103,104</sup>

## Impact of lignin properties and modification on structure–property–performance

### Impact of lignin structure

Lignin's feedstock origin and extraction method determine its structural parameter, which includes syringyl/guaiacyl (S/G) ratio, molecular weight distribution, and functional group content. This in turn governs carbon yield, conductivity, redox activity, and ionic transport. These relationships provide the mechanistic basis for rational lignin selection in specific battery roles.<sup>106</sup>

Hardwood-derived organosolv lignins (S-rich, low sulfur/ash) typically depolymerize more readily, producing homogeneous aromatic domains and mesoporous carbons at moderate carbonization temperatures ( $\approx 700\text{--}900\text{ }^\circ\text{C}$ ). These features favor hard-carbon anodes with high reversible capacity and accessible ion storage sites.<sup>107</sup> In contrast, softwood kraft lignins (G-rich, more condensed) undergo stronger cross-linking *via* C–C condensation pathways, yielding higher char and more graphitizable domains at elevated temperatures ( $>900\text{ }^\circ\text{C}$ ). This enhances electronic conductivity and rate capability, though sometimes at the expense of pseudocapacitive surface functionality.<sup>107,108</sup> Such contrasts explain why organosolv-derived carbons often show higher first-cycle capacity, while kraft-derived carbons excel in rate performance and cycling stability. Reported discrepancies across studies can be reconciled by differences in fractionation, activation/chemical treatment, and carbonization profiles.

Lignosulfonates and soda lignins, with their sulfonate groups and water solubility, are particularly useful in binder and separator applications due to good wetting, film formation, and polymer compatibility.<sup>109</sup> However, residual sulfur and high oxygenated group content complicate graphitization, often requiring purification or tailored activation to achieve high conductivity. Their demonstrated effectiveness as binders for hard-carbon anodes highlights their utility even if they are less suitable as direct precursors for conductive carbons without modification.<sup>109</sup>

Molecular weight strongly influences processing and composite uniformity. Low-MW lignins ( $<2\text{ kDa}$ ) disperse well in polymers such as PAN, PEO, or PVDF, producing smooth, defect-free films with strong adhesion, critical for binder and separator performance.<sup>110</sup> High-MW or highly condensed lignins, by contrast, disrupt polymer packing, induce phase separation, and weaken mechanical strength, compromising electrode integrity during cycling.<sup>109,110</sup>

Taken together, lignin's heterogeneity is both a challenge and an opportunity. By tailoring S/G ratio, molecular weight, and functional-group composition, researchers can optimize carbon yield, conductivity, redox activity, and ionic transport across anodes, cathodes, binders, separators, and electrolytes.

### Impact of lignin fractionation

Fractionation has emerged as a critical strategy to mitigate the variability of lignin by narrowing molecular weight distributions, enriching specific functional groups, and improving batch-to-batch reproducibility. Despite being briefly mentioned in prior sections, its implications for electrochemical performance merit deeper analysis.<sup>111,112</sup>

Among reported fractionation techniques, solvent-based fractionation (using ethanol, methanol, acetone, or aqueous dioxane) consistently yields lignin fractions with the most desirable characteristics for battery applications.<sup>113</sup> These methods selectively isolate low- to medium-molecular-weight fractions (typically  $<2\text{--}5\text{ kDa}$ ) with narrower polydispersity indices and higher phenolic hydroxyl content. Such fractions exhibit superior solubility, processability, and interfacial com-

patibility when incorporated into polymer matrices or used as carbon precursors.<sup>113–115</sup> In contrast, unfractionated kraft lignin contains a broad distribution of condensed, high-molecular-weight species that hinder uniform film formation and lead to inconsistent electrochemical behavior.<sup>116</sup>

For electrode binders and polymer electrolytes, low-molecular-weight, phenolic-rich lignin fractions are particularly advantageous.<sup>117</sup> These fractions form homogeneous blends with polymers such as PEO, PAN, or PVP, enhancing adhesion to active materials and current collectors while maintaining mechanical integrity during cycling.<sup>118</sup> Narrow molecular weight distributions reduce phase separation and cracking, which directly improves capacity retention and coulombic efficiency.<sup>119</sup> These effects are consistent with the stable cycling behavior observed in lignin-based separators and electrolytes summarized in Tables 8 and 9.

In carbonized anode and cathode materials, fractionation improves both carbon yield consistency and microstructural control.<sup>120,121</sup> Low-MW lignin fractions carbonize more uniformly, producing carbons with predictable pore size distributions and defect densities. This uniformity reduces variability in SEI formation and  $\text{Li}^+$  diffusion pathways, helping explain why some lignin-derived carbons exhibit excellent cycling stability while others show rapid capacity fading (Table 5).<sup>121,122</sup> High-molecular-weight, highly condensed fractions, by contrast, tend to generate irregular pore structures and electrically isolated domains, contributing to poor rate performance and low initial coulombic efficiency.<sup>122–124</sup>

Importantly, fractionation also enables application-specific lignin selection. Phenolic-rich, low-MW fractions are optimal for redox-active cathodes and polymer electrolytes, where functional group accessibility governs charge storage and ionic transport. Medium-MW fractions with moderate condensation are better suited for binder and separator applications, where mechanical strength and adhesion dominate. Highly condensed, high-MW fractions, often considered waste streams, may still be valuable for structural carbons or as inactive fillers but are less suitable for electrochemically active roles.<sup>125</sup>

Overall, lignin fractionation should be viewed not as an optional preprocessing step but as a necessary materials engineering tool for producing battery-grade lignin. By reducing structural variability, fractionation directly addresses reproducibility challenges, improves performance consistency, and enhances scalability, key requirements for translating lignin-based materials from laboratory studies to industrial lithium-ion battery manufacturing.<sup>111</sup>

### Impact of lignin modification

A detailed examination of the electrochemical results summarized in Tables 5–9 reveals several consistent structure–property–performance correlations across lignin-based anodes, cathodes, separators, and electrolytes. These trends clarify how specific modification strategies, processing conditions, and microstructural features govern the performance of lignin-derived materials in lithium-ion batteries. Importantly, these insights move beyond descriptive cataloging to provide a



comparative and mechanistic interpretation of the available literature, as expected for a critical review.

For lignin-derived anodes (Table 5), modification strategies involving heteroatom doping, mesopore engineering, and composite formation produce the most significant capacity enhancements. For example, pristine carbonized lignin (CLN) delivers a relatively modest capacity of 350 mAh g<sup>-1</sup> at 750 °C due to its limited conductivity and low carbon yield.<sup>12</sup> When lignin is processed through a MOF-templating route (CMLN), the resulting mesoporous carbon achieves a substantially higher capacity of 560 mAh g<sup>-1</sup>, accompanied by an enhanced Li-ion diffusion coefficient (6.51 × 10<sup>-12</sup> cm<sup>2</sup> s<sup>-1</sup>) due to its increased accessible surface area and hierarchical porosity.<sup>97</sup> The most dramatic performance improvements arise from silicon-modified lignin carbon nanofibers (CNF/Si), where increasing the Si content from 5% to 15% raises the capacity from 439 mAh g<sup>-1</sup> to 921 mAh g<sup>-1</sup>, although high Si loadings reduce capacity retention (94.49% at 5% Si vs. 75.4% at 15% Si) due to fiber distortion, inhomogeneous morphology, and excessive SEI formation on unstable interfaces.<sup>98</sup> These observations collectively indicate that introducing microstructural complexity (e.g., Si domains, MOF-templated pores) enhances capacity and kinetics but must be balanced with structural stability considerations.

A consistent dependence on carbonization temperature is also evident across studies. For instance, in the lignin/PAN-derived carbon fibers (LPCF), increasing the carbonization temperature from 800 °C to 1000 °C increases the reversible capacity from 143 to 267 mAh g<sup>-1</sup> and improves cycling stability (up to 90% retention after 100 cycles), owing to greater graphitic ordering and improved charge transport pathways at higher temperatures.<sup>99</sup> However, this improvement is offset by a reduction in initial coulombic efficiency (ICE), as higher-temperature carbons possess a larger accessible surface area that promotes irreversible SEI formation. These trends reinforce the well-established trade-off between structural ordering and surface-driven side reactions in biomass-derived carbons.<sup>126,127</sup>

Similar structure–performance relationships are observed in lignin-based cathodes (Table 6). Conductivity-enhancing modifications, including PEDOT incorporation and blending with carbon black (C65), consistently produce higher reversible capacities and improved cyclability compared with unmodified lignin cathodes. For example, the lignin/PEDOT (20 : 80) composite delivers 82–92 mAh g<sup>-1</sup> across different electrolytes, while the ternary lignin/PEDOT/C65 composite increases the discharge capacity to 119 mAh g<sup>-1</sup>, demonstrating the synergistic role played by conductive frameworks in facilitating charge transport within the inherently insulating lignin matrix.<sup>103</sup> In contrast, hydrolysis lignin used in primary lithium batteries exhibits a much higher capacity (445 mAh g<sup>-1</sup>). Still, it lacks long-term cycling ability due to its poor intrinsic conductivity and a strong dependence on electrolyte formulation.<sup>104</sup> These contrasting results illustrate that while lignin's quinone-based redox activity can deliver high theoretical

capacity, long-term performance requires the careful modulation of the electronic microstructure.<sup>71,104</sup>

For separators (Table 8), porosity and microstructural continuity emerge as dominant determinants of ionic conductivity and rate capability. Lignin/PAN electrospun membranes with well-distributed interconnected pores achieve ionic conductivities as high as 1.24 × 10<sup>-3</sup> S cm<sup>-1</sup> and exhibit strong rate performance (capacity retention >90% across 0.2–1 C), attributed to enhanced electrolyte uptake and minimized tortuosity. However, increasing lignin content beyond optimal ratios leads to phase separation and weakened mechanical integrity, reducing separator performance, highlighting the importance of polymer–lignin compatibility in membrane design.

Finally, lignin-based electrolytes (Table 9) show that polymer network flexibility and the presence of ion-coordinating functional groups strongly govern ionic conductivity. The lignin/PVP-based gel polymer electrolyte (LP-GPE), modified with KH-550 silane, achieves the highest conductivity (2.52 × 10<sup>-3</sup> S cm<sup>-1</sup>) and near-complete capacity retention (99%), significantly outperforming other lignin-based systems. This improvement can be attributed to enhanced segmental motion and increased Li<sup>+</sup> coordination resulting from silane cross-linking and optimized lignin : PVP ratios. In contrast, lignin/poly(*N*-vinylimidazole-*co*-PEGMA) membranes exhibit lower conductivity (2.6 × 10<sup>-4</sup> S cm<sup>-1</sup>) due to their denser network and reduced free volume for ion transport.

Across all components, the trends in Tables 5–9 clearly demonstrate that lignin's electrochemical performance is fundamentally governed by the interplay between microstructure (porosity, graphitization), chemical functionality (quinone groups, heteroatom content), and compositional design (polymer matrices, Si loading, conductive additives). Modification strategies that increase electronic conductivity, stabilize pore architecture, or enhance Li<sup>+</sup> mobility consistently produce superior performance.<sup>108,123</sup> Conversely, approaches that lead to excessive surface area, phase separation, or structural instability result in poor initial CE, accelerated capacity fading, or compromised mechanical durability.<sup>126,127</sup> These correlations provide actionable guidelines for optimizing lignin-derived battery components and highlight the mechanistic basis underlying divergent results reported in the literature Table 10.

## Life cycle assessment (LCA), solvent footprints, and toxicity of lignin

Despite repeated claims that lignin is a more sustainable feedstock for battery components, there is a striking shortage of direct, comparable life-cycle evidence for lignin-derived battery materials in the public literature. Recent reviews and process studies emphasize that the environmental benefit of lignin materials is not automatic. It depends entirely on the chosen extraction, fractionation, chemical modification, and high-temperature processing pathways.<sup>132</sup>



Table 10 Comparative summary of lignin sources

Lignin source	Typical composition and impurities	Observed carbon/material properties	Post-treatments/typical processing	Recommended battery role(s)	Ref.
Organosolv lignin	Higher S/G ratio, lower ash/sulfur content, clean feedstock	Produces porous carbon; oxygen-doped hierarchical porous carbons High surface area, redox oxygen functionalities	Activation + carbonization; sometimes blending (e.g., MOF templating) for porosity	Hard carbon anodes (especially for high capacity)  Porous carbons for electrodes/separators	46,64 and 128
Kraft lignin	G-rich, more condensed aromatic structure, some sulfur content/residues depending on purification	When carbonized, it can yield carbons with a high BET surface area  Good porosity and electrochemical double-layer behavior	Carbonization (600–1000 °C) + meso/micro-porosity tuning  Sometimes used as a binder or composite matrix	Electrochemical capacitors, electrodes where porosity and surface area are critical  Candidates for high-rate anodes if graphitized or doped appropriately.	12,129 and 130
Lignosulfonate/soda lignin	Lower molecular weight, more polar/oxygenated or sulfonated groups	Carbonization up to 1400 °C  Produce carbon with high electrical conductivity	High-temperature carbonization, sometimes with purification/desulfonation or activation Careful removal of impurities is often required	Binders, separators, conductive fillers, composite matrices	131
Mixed/technical lignins  (unfractionated)	Mixed S/G ratio; broad MW and impurity distribution; high heterogeneity	Carbon performance is variable; performance heavily depends on purification/fractionation	Recommended to fractionate (solvent, membrane, precipitation) before carbonization; then activation	Depending on the fraction obtained, porous carbons, binders, and anodes are used. But only after fractionation and careful processing.	121

A small number of LCA studies and industrial disclosures suggest that well-designed lignin-based carbon routes can deliver low global warming potential (GWP) per kg of carbon product.<sup>133</sup> For example, life-cycle studies of certain lignin-based carbon fibre routes report very low cradle-to-gate climate impacts ( $\approx 1.5$  kg CO<sub>2</sub>-eq per kg for lignin-based carbon fibres *versus*  $\approx 38.9$  kg CO<sub>2</sub>-eq per kg for fossil-based carbon fibres),<sup>133,134</sup> a dramatic difference that largely reflects feedstock substitution and lower process emissions when optimized. Similarly, techno-economic/LCA modeling of biochar to biographite routes reports GWP values in the  $\sim 2$ – $3$  kg CO<sub>2</sub>-eq per kg range for converted graphitic materials under favorable process configurations.<sup>134</sup>

By contrast, published LCAs for commercial graphite production (natural or synthetic) show a wide range of GWP values, from very low ( $\leq \sim 1.2$  kg CO<sub>2</sub>-eq per kg in optimized synthetic graphite routes reported by some manufacturers) to much higher footprints ( $\geq 10$ – $17$  kg CO<sub>2</sub>-eq per kg in some conventional supply chains), depending on ore quality, electricity mix, and purification intensity.<sup>133</sup> These widespread results highlight that comparability requires carefully matched system boundaries and consistent allocation rules.

Lignin-based battery systems can reduce upstream mining and mineral processing emissions. Still, they introduce other potentially large burdens: (i) thermal energy for carbonization (temperatures up to 800–1400 °C are common) can dominate GWP unless low-carbon heat sources are used; (ii) chemical activation and doping (KOH, acids, sulfonation reagents) and

solvent-based fractionation (organic solvents, DMF, DMAC, NMP alternatives) can add substantial environmental and toxicity burdens if not recycled; and (iii) lower initial coulombic efficiency and higher irreversible loss (observed for many lignin-derived carbons) can reduce cell-level performance and therefore erode any material-level GWP advantage when translated to per-kWh metrics.<sup>135</sup> Several recent analyses caution that aggressive chemical activation or energy-intensive processing can eliminate the raw material advantage of biomass-derived precursors.<sup>132</sup>

The electrode manufacturing stage is another important lever: *N*-methyl-2-pyrrolidone (NMP), commonly used with PVDF binders, is a high-impact solvent (toxicity, occupational hazard, and life-cycle impact), and strategies that enable water-based slurries or low-toxicity solvent systems materially reduce life cycle impacts of electrode manufacture.<sup>136</sup> Lignin fractions that allow aqueous processing (*via* water-soluble lignosulfonates or tailored fractionation), therefore, provide a distinct cradle-to-gate benefit, but only if solvent recovery and process emissions are accounted for. Published studies show electrode production impacts fall when NMP is avoided or substantially recovered in solvent recovery systems.<sup>136,137</sup>

Toxicity and ecotoxicity considerations are also important. Native lignin (including kraft and organosolv fractions) and widely used technical lignins (e.g., lignosulfonates) are generally low in acute mammalian toxicity and have long histories of industrial use (e.g., lignosulfonates in adhesives and road binders), but their environmental footprint depends on



**Table 11** Representative life cycle GWP for lignin derivatives

Route/material	Reported GWP (kg CO <sub>2</sub> -eq per kg)	Key assumptions/notes	Ref.
Lignin-based carbon fiber (optimized pilot route)	1.50	Cradle-to-gate; favorable allocation of lignin as pulp by-product;	132
Lignin-CF (integrated redissolution spinning; energy-intensive)	20.7–25.3	Includes solvent/IL use and energy-intensive spinning;	142
Lignin-derived hard carbon (modelled for SIB anode)	Not reported	sensitivity to electricity	143
Hazelnut shell / bio-waste hard carbon	2–5 (varies by study)	LCA values depend on pyrolysis energy and allocation rules; some bio-waste HC routes report low-to-moderate GWP.	144
Soda lignin (high-temperature) carbon (lab/pilot)	Not reported	High-temperature graphitization ( $\geq 1400$ °C) GWP depends on the heat source	144

functionalization and residual processing chemicals (e.g., sulfur residues, sulfonating agents, acid catalysts, solvents).<sup>138</sup> By-products (e.g., acid hydrolysis liquor, solvent residues, spent activation reagents) can pose toxicity and disposal burdens that must be accounted for.<sup>138</sup>

To substantiate sustainability claims, it is suggested that future lignin-battery studies include at minimum: (i) a cradle-to-gate LCA with transparent system boundaries and allocation rules comparing lignin-derived carbon with synthetic and natural graphite on a per-kg and per-kWh basis; (ii) explicit accounting for carbonization energy (including heat source CO<sub>2</sub> intensity), solvent use and solvent recovery rates, activating reagent stoichiometry and fate, and initial coulombic efficiency (ICE) losses translated into cell-level energy and emissions; (iii) a basic ecotoxicity/safety profile for process waste streams; and (iv) sensitivity scenarios showing how switching to renewable heat or solvent recycling changes outcomes.<sup>139</sup> Where possible, research should report data in a standardized format (GWP kg CO<sub>2</sub>-eq per kg product; GWP kg CO<sub>2</sub>-eq per kWh cell; water use L kg<sup>-1</sup> product; and key toxicity metrics for process effluents).<sup>139,140</sup>

Lignin-derived battery materials have demonstrable potential to reduce life-cycle greenhouse-gas impacts if low-energy processing, minimal use of hazardous solvents, solvent recovery, and moderate activation protocols are used. However, aggressive activation and high-temperature graphitization without low-carbon heat sources can negate feedstock advantages.<sup>134</sup> Because of the heterogeneity of published LCA and industrial data, claims of “CO<sub>2</sub> emission reduction with lignin utilization” should be presented with caveats and the system-level metrics as suggested above.<sup>141</sup> Table 11 summarizes the life cycle GWP (kg CO<sub>2</sub>-eq per kg product) for lignin derivatives.

## Recyclability and end-of-life considerations

The incorporation of lignin into lithium-ion battery components introduces new considerations for recycling and end-of-life management, which are highly relevant from a green chemistry and circular economy perspective.<sup>145</sup> Although sys-

tematic recycling studies on lignin-containing lithium-ion batteries remain limited, several conceptual advantages and challenges can be identified when compared to conventional batteries based entirely on petroleum-derived polymers.<sup>146</sup>

In traditional lithium-ion batteries, recycling processes primarily rely on pyrometallurgical and hydrometallurgical routes to recover valuable metals, while polymeric binders (e.g., PVDF), separators, and electrolytes are largely combusted or discarded due to their chemical stability and limited recyclability.<sup>147,148</sup> In contrast, lignin-based components introduce oxygen-rich, aromatic biopolymers that are inherently more amenable to thermal decomposition, chemical solvolysis, or biological degradation. As a result, lignin-based binders, separators, and polymer electrolytes may facilitate cleaner thermal removal during electrode delamination and metal recovery, potentially reducing the need for aggressive solvents, such as *N*-methyl-2-pyrrolidone (NMP).<sup>149,150</sup>

From a hydrometallurgical perspective, replacing fluorinated binders with lignin-based alternatives could reduce the formation of hazardous fluorinated by-products and simplify downstream aqueous processing. Moreover, lignin's natural affinity for metal ions raises the possibility of designing future lignin-based components that actively assist in metal recovery through chelation or selective dissolution, although this concept remains largely unexplored.<sup>151</sup>

However, the introduction of lignin also presents challenges. Variability in lignin composition, molecular weight, and functional group distribution may influence decomposition behavior and residue formation during recycling.<sup>152,153</sup> Additionally, carbonized lignin used in anodes or conductive additives is chemically similar to other hard carbons. It therefore does not significantly alter existing recycling workflows for carbonaceous materials.<sup>154</sup> Consequently, the primary recycling benefits of lignin integration are expected to arise from its use in non-active components, such as binders, separators, and polymer electrolytes, rather than from carbonized electrode materials.

Overall, while lignin-containing lithium-ion batteries are not expected to require fundamentally new recycling technologies, their integration offers opportunities to simplify binder removal, reduce toxic emissions, and improve the environmental footprint of battery recycling.<sup>108</sup>



## Commercialization status of lignin-based battery components

Despite extensive academic research on lignin-based materials for lithium-ion batteries, large-scale commercial deployment remains limited. To date, the most notable example is Stora Enso's lignin-derived hard carbon (Lignode®), which has reached pilot-scale production and has been evaluated as an anode material for lithium-ion and sodium-ion batteries.<sup>69,104,155</sup> This development demonstrates the technical feasibility of converting industrial lignin streams into battery-grade carbon while maintaining compatibility with existing electrode manufacturing processes.

Beyond Stora Enso, several pre-commercial and near-commercial efforts have been reported,<sup>155</sup> particularly in non-active battery components. Multiple research groups and industrial consortia have explored lignin-based binders and conductive additives as potential replacements for poly(vinylidene fluoride) (PVDF), motivated by the desire to eliminate fluorinated polymers and toxic solvents such as *N*-methyl-2-pyrrolidone. While these materials have not yet reached widespread commercialization, their compatibility with aqueous processing and conventional slurry-coating techniques positions them as strong candidates for industrial adoption.

In separators and polymer electrolytes, lignin-based membranes remain at the laboratory and pilot scale, primarily due to challenges associated with mechanical robustness, long-term electrochemical stability, and moisture sensitivity.<sup>156,157</sup> Nevertheless, the use of lignin as a functional additive rather than a primary structural component has shown promise in improving electrolyte uptake, ionic conductivity, and interfacial stability, suggesting potential for incremental industrial integration.<sup>152</sup>

Overall, current commercialization efforts indicate that lignin's most realistic near-term impact lies in hybrid or auxiliary roles, such as hard carbon anodes derived from industrial lignin streams and bio-based binders or additives in electrodes.<sup>158</sup> Full replacement of conventional battery materials by lignin remains unlikely in the short term; however, continued advances in fractionation, processing control, and life-cycle optimization are expected to accelerate the transition from pilot-scale demonstrations to industrial adoption.

## Current and future trends of lignin in lithium-ion batteries

Lignin-based materials have emerged as promising candidates for sustainable energy storage applications, particularly in lithium-ion batteries, due to lignin's abundance, low production cost, and functional versatility. However, their widespread adoption remains hindered by several fundamental challenges, most notably, the intrinsic structural heterogeneity of lignin. Lignin's chemical structure varies significantly depending on the botanical source (*e.g.*, hardwood, softwood,

or grasses) and the extraction method (*e.g.*, kraft, organosolv, soda, or sulfite pulping).<sup>159,160</sup> For instance, hardwood lignin is typically rich in syringyl (S) units, while softwood lignin contains predominantly guaiacyl (G) units, which impacts its reactivity, thermal stability, and electronic properties.<sup>14</sup>

Moreover, the production process parameters, such as temperature, pH, and chemical treatment, influence the degree of condensation, molecular weight, and functional group distribution (*e.g.*, methoxy, hydroxy, carbonyl). These structural disparities can lead to batch-to-batch variability in performance when lignin is used as a component in electrodes, binders, separators, or electrolytes.<sup>161</sup> For example, variations in hydroxy group content may affect hydrogen bonding and adhesion, while differences in molecular weight and branching impact solubility and film-forming behavior. This inconsistency presents a major obstacle to scaling lignin-based components for commercial battery manufacturing.

To address the problem of heterogeneity, researchers have explored fractionation techniques, such as solvent-based fractionation, ultrafiltration, and pH-based separation, to isolate more uniform lignin fractions. These methods help improve the homogeneity of lignin in terms of molecular weight and functional group distribution, which can enhance its reactivity and compatibility in composite materials.<sup>162,163</sup> Another promising approach is the conversion of lignin into nanoparticles. Nanoscale lignin offers a higher surface area, improved dispersibility in polymer matrices, and more consistent behavior during electrochemical cycling. Lignin nanoparticles (LNPs) have been shown to improve the mechanical and thermal stability of membranes and electrodes, while enabling more uniform morphology in composite structures.<sup>163</sup>

Additionally, lignin suffers from inherently low electronic and ionic conductivity, which limits its utility as an active electrode material or electrolyte component without further chemical modification or blending with conductive polymers or nanomaterials.<sup>164</sup> Addressing both the structural variability and functional limitations of lignin is thus essential for realizing its full potential in next-generation, bio-derived energy storage systems.

For lignin to function effectively as an electrolyte, it must exhibit high ionic conductivity ( $\geq 10^{-3}$  S cm<sup>-1</sup>) to ensure efficient lithium transport.<sup>101</sup> Additionally, it requires a broad electrochemical stability window ( $>4.5$  V *vs.* Li/Li<sup>+</sup>) to remain stable under high-voltage operation, along with a high lithium transference number ( $>0.5$ ) to minimize charge transport resistance.<sup>102</sup> As a separator, lignin must possess high porosity, allowing for rapid ion diffusion, while maintaining strong mechanical stability to prevent lithium dendrite formation.<sup>165</sup> Thermal resistance is also critical to ensure safety in high-power applications. If used as an electrode, the lignin should have high electronic conductivity, structural robustness, and redox-active functional groups to enhance lithium-ion storage capacity and cycling performance.<sup>166</sup> As a cathode, it must exhibit a high specific capacity ( $>150$  mAh g<sup>-1</sup>), enabling sufficient energy storage, and a high working potential ( $>3.4$  V *vs.* Li/Li<sup>+</sup>) to ensure high energy density. It should also possess



good electronic conductivity ( $>10^{-4}$  S cm $^{-1}$ ) or be combined with conductive additives to reduce internal resistance. Furthermore, structural stability is essential to minimize volume change ( $<5\%$ ) during cycling, to prevent electrode degradation.<sup>167</sup> For anodes, lignin-derived carbons should have a low working potential (0.1–1.0 V vs. Li/Li $^{+}$ ) and a high specific capacity ( $>300$  mAh g $^{-1}$ ) to maximize cell voltage. High electrical conductivity ( $>10^{-3}$  S cm $^{-1}$ ) is important for fast charge/discharge, while mechanical integrity helps withstand repeated lithiation/delithiation without structural failure. Fast lithium-ion diffusion coefficients ( $>10^{-14}$  cm $^2$  s $^{-1}$ ) are needed to ensure good rate capability.<sup>42</sup> Without these characteristics, lignin's application in lithium-ion batteries would be fundamentally limited.

To address the poor ionic conductivity of lignin, chemical functionalization is commonly employed to introduce ion-exchangeable groups that improve its ability to facilitate lithium-ion transport. Among the most studied functional groups, sulfonic acid groups ( $-\text{SO}_3\text{H}$ ) and carboxylic acid groups ( $-\text{COOH}$ ) are particularly noteworthy. Sulfonation introduces fixed anionic sites within the lignin backbone, significantly enhancing ion dissociation and lithium-ion conductivity. Sulfonated lignin-based materials have demonstrated ionic conductivities surpassing that of commercial membranes, *e.g.*, Nafion, in hydrated thin films.<sup>168</sup> In contrast, the incorporation of  $-\text{COOH}$  groups primarily increases the hydrophilicity and compatibility of lignin with polar electrolytes and polymer matrices. However, due to their weaker acidity and lower degree of ion dissociation, carboxylic groups offer limited improvement in ion transport compared to sulfonic groups.<sup>162</sup> Therefore, sulfonation is generally considered more effective in enhancing the electrochemical performance of lignin-based materials for lithium-ion battery applications, especially when ionic mobility is critical.<sup>169</sup> Quaternary ammonium ( $-\text{N}^+\text{R}_3$ ) can further improve ion transport by immobilizing anions, thereby increasing lithium-ion transfer number and reducing polarization.<sup>170</sup> However, these cationic sites are often chemically unstable at high voltages, and their incorporation may lead to phase separation or compatibility issues with anionic lithium salts.<sup>170</sup> Additionally, phosphorylation ( $-\text{PO}_4^{3-}$ ) modifications can enhance lithium salt solubility, improving the lignin's compatibility with conventional liquid electrolytes.<sup>171</sup> But their bulky structure may hinder uniform dispersion within polymer matrices and could lead to rigidity and reduced segmental mobility, thereby limiting ionic conductivity under low-temperature conditions.<sup>172</sup> These functional groups create ionic pathways within the lignin, transforming it into a viable component for the solid-state and gel polymer electrolytes, where efficient ion transport is essential.<sup>173</sup>

While functionalization addresses the ionic conductivity of lignin, hybridization with conductive materials is crucial to improving its electronic conductivity, especially when lignin is used as an active material or conductive additive in lithium-ion battery anodes. For instance, incorporating graphene or carbon nanotubes (CNTs) into lignin matrices creates continu-

ous conductive networks that enhance electron mobility throughout the electrode structure.<sup>174</sup> This significantly improves rate performance and charge-discharge kinetics. Such lignin-carbon hybrids have been successfully applied in lithium-ion battery anodes, where they deliver higher capacities, better cycling stability, and improved electrical conductivity compared to pristine lignin.<sup>175</sup> Another effective approach is to coat lignin with conductive polymers. This not only enhances electronic conductivity but also provides mechanical flexibility, improving material durability under cycling conditions.<sup>176</sup> Furthermore, carbonizing the lignin at high temperatures (800–1000 °C) converts it into a highly porous carbon structure, significantly boosting its conductivity and making it suitable for high-capacity cathodes and supercapacitor electrodes.<sup>177</sup> These hybridization strategies allow the lignin to retain its sustainable and low-cost advantages while achieving conductivity levels necessary for use in high-performance electrodes and conductive binders.

The integration of lignin into lithium-ion battery components is motivated not only by sustainability considerations but also by the potential to mitigate specific limitations associated with conventional battery materials.<sup>12</sup> However, the effectiveness of lignin in addressing these shortcomings varies significantly depending on the component and mode of incorporation.<sup>152,178</sup>

In electrode binders, lignin-based materials offer clear advantages over conventional fluorinated binders such as PVDF. Lignin enables aqueous processing, eliminating the need for toxic and high-boiling solvents such as *N*-methyl-2-pyrrolidone, while also providing strong adhesion through abundant hydroxyl and aromatic functionalities. These properties improve electrode integrity during cycling and reduce environmental and health impacts without sacrificing electrochemical performance, making lignin a particularly compelling alternative in this application.

For anode materials, lignin-derived hard carbons partially address the sustainability and cost limitations of synthetic graphite by utilizing renewable feedstocks and lower carbonization temperatures. In addition, their larger interlayer spacing and disordered structure can enhance lithium storage capacity and rate capability.<sup>179</sup> However, lignin-based hard carbons do not fully resolve issues related to initial coulombic efficiency and long-term cycling stability, which remain inferior to highly optimized graphite anodes. As such, lignin-based carbons should be viewed as complementary rather than direct drop-in replacements at the current stage of development.<sup>180</sup>

In cathode materials, lignin contributes redox-active quinone functionalities that enable faradaic charge storage.<sup>181</sup> This feature introduces new charge-storage mechanisms beyond traditional intercalation. Nevertheless, the intrinsically low electronic conductivity of lignin limits its standalone cathode performance, necessitating conductive polymer or carbon additives. Thus, lignin enhances functionality but does not eliminate the need for conductive frameworks.<sup>149</sup>

For separators and electrolytes, lignin incorporation improves electrolyte uptake, thermal stability, and interfacial



compatibility due to its polar functional groups. In gel polymer electrolytes, lignin enhances ionic conductivity and mechanical flexibility when combined with appropriate polymer matrices. However, lignin-based electrolytes have yet to match the wide electrochemical stability window and high conductivity of state-of-the-art liquid electrolytes, indicating that further optimization is required.<sup>182</sup>

Overall, lignin does not represent a universal solution to all lithium-ion battery limitations. Instead, its greatest value lies in targeted roles where its chemical functionality, processability, and renewability directly address specific shortcomings—particularly in binders, separators, and auxiliary components. When strategically integrated, lignin can improve environmental performance and processing safety while maintaining competitive electrochemical functionality, thereby offering a balanced pathway toward more sustainable lithium-ion battery systems.<sup>183</sup>

In summary, to develop lignin into a competitive material for lithium-ion batteries, modifications should be tailored to its specific function within the battery system. In cathodes, hybridizing with graphene, CNTs, and conductive polymers can enhance conductivity while maintaining structural integrity. For anode and conductive binder applications, carbonization of lignin can create a highly conductive, high surface area material, improving charge storage and cycling stability. For electrolytes and separators, functionalization with sulfonic acid and quaternary ammonium groups should be prioritized to enhance ionic conductivity, while a porous polymer matrix can improve electrolyte retention. By integrating chemical functionalization and hybridization, the lignin can be transformed into a high-performance material, suitable for diverse applications within lithium-ion batteries, offering a sustainable, cost-effective, and scalable alternative to conventional battery components.

## Conclusions

Lignin represents a compelling and versatile bio-based platform for the development of more sustainable lithium-ion battery components, offering advantages rooted in its abundance, renewability, aromatic structure, and chemically tunable functional groups. As demonstrated throughout this review, lignin's value extends beyond the role it plays as a carbon precursor, enabling multifunctional contributions across active and non-active battery components when appropriately processed and engineered.

A central conclusion of this work is that the performance variability reported for lignin-based battery materials is primarily governed by lignin heterogeneity, including source-dependent structure, molecular weight distribution, and functional group chemistry. Comparative analysis across studies reveals that parameters such as S/G ratio, degree of condensation, and fractionation critically influence carbon yield, porosity development, interfacial behaviour, and electrochemical stability. Fractionation strategies that narrow mole-

cular weight distributions and tailor functional group content emerge as essential steps toward achieving reproducible, battery-grade lignin materials.

In anode applications, lignin-derived hard carbons offer promising specific capacities and rate performance, particularly when integrated into hybrid architectures with silicon, graphene, or conductive polymers. However, challenges related to initial coulombic efficiency, SEI stability, and long-term cycling durability remain key obstacles relative to mature graphite anodes. In cathode systems, lignin's quinone-type redox activity introduces alternative charge-storage mechanisms, though low intrinsic electronic conductivity necessitates conductive frameworks for practical implementation.

The most immediate and impactful applications of lignin are found in auxiliary battery components, including binders, separators, and polymer electrolytes. In these roles, lignin directly addresses several limitations of conventional petroleum-derived materials by enabling aqueous processing, eliminating fluorinated binders, enhancing thermal stability, and improving electrolyte uptake. From a green chemistry perspective, these advantages translate into reduced solvent toxicity, lower processing energy, and improved recycling compatibility.

Importantly, lignin does not constitute a universal replacement for all conventional battery materials. Rather, its greatest potential lies in targeted integration, where its chemical functionality and processability align with specific performance and sustainability requirements. Continued progress will depend on standardizing lignin fractionation, advancing structure–property–performance understanding, and developing hybrid material systems that balance electrochemical performance with environmental and economic viability. Addressing these challenges will be critical for positioning lignin as a scalable, multifunctional contributor to next-generation, low-carbon lithium-ion battery technologies.

## Author contributions

E. Aidoo: data analysis, manuscript preparation – first draft. P. Fatehi: supervision, manuscript preparation – revision, funding.

## Conflicts of interest

The authors declare no conflicting interests.

## Data availability

Data are provided within the manuscript. No primary research results, software or code have been included, and no new data were generated or analysed as part of this review.



## Acknowledgements

The authors would like to thank the Canada Research Chairs program and NSERC Canada for their support.

## References

- C. Liu, F. Li, L. Ma and H. Cheng, *Adv. Mater.*, 2010, **22**, E28–E62.
- J. B. Goodenough, *Energy Storage Mater.*, 2015, **1**, 158–161.
- Y. Li, Y. Lu, C. Zhao, Y.-S. Hu, M.-M. Titirici, H. Li, X. Huang and L. Chen, *Energy Storage Mater.*, 2017, **7**, 130–151.
- R. Holze, *J. Solid State Electrochem.*, 2015, **19**, 1253–1253.
- J. Cho, Z. Chen, S. A. Freunberger, X. Ji, Y. K. Sun, K. Amine, G. Yushin, N. F. Nazar, J. Chao and P. G. Bruce, *Angew. Chem.*, 2012, **51**, 9994–10024.
- J. B. Goodenough and Y. Kim, *Chem. Mater.*, 2010, **22**, 587–603.
- J. B. Goodenough and K.-S. Park, *J. Am. Chem. Soc.*, 2013, **135**, 1167–1176.
- Z. Yang, J. Zhang, M. C. W. Kintner-Meyer, X. Lu, D. Choi, J. P. Lemmon and J. Liu, *Chem. Rev.*, 2011, **111**, 3577–3613.
- M. Armand and J.-M. Tarascon, *Nature*, 2008, **451**, 652–657.
- J. Liu, J. Zhang, Z. Yang, J. P. Lemmon, C. Imhoff, G. L. Graff, L. Li, J. Hu, C. Wang, J. Xiao, G. Xia, V. V. Viswanathan, S. Baskaran, V. Sprenkle, X. Li, Y. Shao and B. Schwenzer, *Adv. Funct. Mater.*, 2013, **23**, 929–946.
- I. Dobryden, C. Montanari, D. Bhattacharjya, J. Aydin and A. Ahniyaz, *Materials*, 2023, **16**, 5553.
- M. Baloch and J. Labidi, *RSC Adv.*, 2021, **11**, 23644–23653.
- J. Zakzeski, P. C. A. Bruijninx, A. L. Jongerius and B. M. Weckhuysen, *Chem. Rev.*, 2010, **110**, 3552–3599.
- S. Laurichesse and L. Avérous, *Prog. Polym. Sci.*, 2014, **39**, 1266–1290.
- W. O. S. Doherty, P. Mousavioun and C. M. Fellows, *Ind. Crops Prod.*, 2011, **33**, 259–276.
- P. Figueiredo, K. Lintinen, A. Kiriazis, V. Hynninen, Z. Liu, T. Bauleth-Ramos, A. Rahikkala, A. Correia, T. Kohout, B. Sarmiento, J. Yli-Kauhala, J. Hirvonen, O. Ikkala, M. A. Kostianen and H. A. Santos, *Biomaterials*, 2017, **121**, 97–108.
- V. K. Thakur, M. K. Thakur, P. Raghavan and M. R. Kessler, *ACS Sustainable Chem. Eng.*, 2014, **2**, 1072–1092.
- R. J. A. Gosselink, E. de Jong, B. Guran and A. Abächerli, *Ind. Crops Prod.*, 2004, **20**, 121–129.
- S.-X. Wang, L. Yang, L. P. Stubbs, X. Li and C. He, *ACS Appl. Mater. Interfaces*, 2013, **5**, 12275–12282.
- H. Luo and M. M. Abu-Omar, in *Encyclopedia of Sustainable Technologies*, ed. M. A. Abraham, Elsevier, Oxford, 2017, pp. 573–585.
- Y. Yi, J. Zhuang, C. Liu, L. Lei, S. He and Y. Hou, *Energies*, 2022, **15**, 9450.
- Y. Tong, J. Yang, J. Li, Z. Cong, L. Wei, M. Liu, S. Zhai, K. Wang and Q. An, *J. Mater. Chem. A*, 2023, **11**, 1061–1082.
- K. Pielichowska and K. Pielichowski, *Prog. Mater. Sci.*, 2014, **65**, 67–123.
- B. Xu, D. Qian, Z. Wang and Y. S. Meng, *Mater. Sci. Eng.*, 2012, **73**, 51–65.
- Y. Li, S. Ding, L. Wang, W. Wang, C. Lin and X. He, *eTransportation*, 2024, **22**, 100368.
- J. R. Joshua, T. Maiyalagan, N. Sivakumar and Y. S. Lee, in *Rechargeable Lithium-Ion Batteries*, CRC Press, 2020.
- Y. Li, S. Wang, Y. Dong, Y. Yang, Z. Zhang and Z. Tang, *Adv. Energy Mater.*, 2020, **10**, 2070013.
- X. Wu, J. Jiang, C. Wang, J. Liu, Y. Pu, A. Ragauskas, S. Li and B. Yang, *Biofuels, Bioprod. Biorefin.*, 2020, **14**, 650–672.
- M. Zhao, J. Wang, C. Chong, X. Yu, L. Wang and Z. Shi, *RSC Adv.*, 2015, **5**, 101115–101120.
- Y. Ma, K. Chen, J. Ma, G. Xu, S. Dong, B. Chen, J. Li, Z. Chen, X. Zhou and G. Cui, *Energy Environ. Sci.*, 2019, **12**, 273–280.
- X. Lin, Y. Liu, H. Tan and B. Zhang, *Carbon*, 2020, **157**, 316–323.
- T. C. Nirmale, B. B. Kale and A. J. Varma, *Int. J. Biol. Macromol.*, 2017, **103**, 1032–1043.
- Y. Zhang, H. Geng, W. Wei, J. Ma, L. Chen and C. C. Li, *Energy Storage Mater.*, 2019, **20**, 118–138.
- M. H. Sipponen, H. Lange, C. Crestini, A. Henn and M. Österberg, *ChemSusChem*, 2019, **12**, 2039–2054.
- W. E. Tenhaeff, O. Rios, K. More and M. A. McGuire, *Adv. Funct. Mater.*, 2014, **24**, 86–94.
- O. Sevastyanova, M. Helander, S. Chowdhury, H. Lange, H. Wedin, L. Zhang, M. Ek, J. F. Kadla, C. Crestini and M. E. Lindström, *J. Appl. Polym. Sci.*, 2014, **131**, 40799.
- R. Kumar, A. Pradeep and P. Bhargava, *Mater. Renew. Sustain. Energy*, 2025, **14**, 20.
- A. Scott, *C&EN Global Enterp.*, 2024, **102**, 15–15.
- M. S. Whittingham, *Chem. Rev.*, 2004, **104**, 4271–4302.
- Y. Mekonnen, A. Sundararajan and A. I. Sarwat, in *SoutheastCon 2016*, vol. 2016, pp. 1–6.
- A. Sarkar, *Multiphysics analysis of electrochemical and electromagnetic system addressing lithium-ion battery and permanent magnet motor*, Iowa State University, Ames, 2018.
- J.-M. Tarascon and M. Armand, *Nature*, 2001, **414**, 359–367.
- T. Ma, S. Wu, F. Wang, J. Lacap, C. Lin, S. Liu, M. Wei, W. Hao, Y. Wang and J. W. Park, *ACS Appl. Mater. Interfaces*, 2020, **12**, 56086–56094.
- J. Wen, Y. Yu and C. Chen, *Mater. Express*, 2012, **2**, 197–212.
- S. Chatterjee, T. Saito, O. Rios and A. Johs, in *ACS Symposium Series*, ed. S. O. Obare and R. Luque, American Chemical Society, Washington, DC, 2014, vol. 1186, pp. 203–218.
- P. Li, S. Wu and Y. Ding, *BioResources*, 2024, **19**, 3979–4000.



- 47 C. Crestini and D. S. Argyropoulos, *J. Agric. Food Chem.*, 1997, **45**, 1212–1219.
- 48 E. J. Son, J. H. Kim, K. Kim and C. B. Park, *J. Mater. Chem. A*, 2016, **4**, 11179–11202.
- 49 G. Milczarek and O. Inganäs, *Science*, 2012, **335**, 1468–1471.
- 50 M. Quan, D. Sanchez, M. F. Wasylkiw and D. K. Smith, *J. Am. Chem. Soc.*, 2007, **129**, 12847–12856.
- 51 H. Wang, P. Feng, F. Fu, X. Yu, D. Yang, W. Zhang, L. Niu and X. Qiu, *Carbon Neutralization*, 2022, **1**, 277–297.
- 52 J.-P. Yen, C.-C. Chang, Y.-R. Lin, S.-T. Shen and J.-L. Hong, *J. Electrochem. Soc.*, 2013, **160**, A1811.
- 53 S.-K. Jung, I. Hwang, D. Chang, K.-Y. Park, S. J. Kim, W. M. Seong, D. Eum, J. Park, B. Kim, J. Kim, J. H. Heo and K. Kang, *Chem. Rev.*, 2020, **120**, 6684–6737.
- 54 S. Zhang, M. He, C.-C. Su and Z. Zhang, *Curr. Opin. Chem. Eng.*, 2016, **13**, 24–35.
- 55 K. Xu, *Chem. Rev.*, 2014, **114**, 11503–11618.
- 56 S. S. Zhang, *J. Power Sources*, 2007, **164**, 351–364.
- 57 M. Irfan, M. Atif, Z. Yang and W. Zhang, *J. Power Sources*, 2021, **486**, 229378.
- 58 M. Winter and J. O. Besenhard, *Electrochim. Acta*, 1999, **45**, 31–50.
- 59 X. Zuo, J. Zhu, P. Müller-Buschbaum and Y.-J. Cheng, *Nano Energy*, 2017, **31**, 113–143.
- 60 J. Christensen and J. Newman, *J. Solid State Electrochem.*, 2006, **10**, 293–319.
- 61 W. Xu, J. Wang, F. Ding, X. Chen, E. Nasybulin, Y. Zhang and J.-G. Zhang, *Energy Environ. Sci.*, 2014, **7**, 513–537.
- 62 J. R. Dahn, T. Zheng, Y. Liu and J. S. Xue, *Science*, 1995, **270**, 590–593.
- 63 N. Nitta, F. Wu, J. T. Lee and G. Yushin, *Mater. Today*, 2015, **18**, 252–264.
- 64 R. Brown, Stora Enso Launches Beyond Board Packaging Services to Support Customers in Navigating Circular Economy Challenges, <https://manufacturingdigital.com/articles/stora-ensos-beyond-board-to-advise-customers-on-packaging>, (accessed 17 December 2025).
- 65 S. Li, W. Luo, Q. He, J. Lu, J. Du, Y. Tao, Y. Cheng and H. Wang, *Int. J. Mol. Sci.*, 2023, **24**, 284.
- 66 M. Culebras, G. A. Collins, A. Beaucamp, H. Geaney and M. N. Collins, *Eng. Sci.*, 2022, **17**, 195–203.
- 67 C. Song, C. Gao, Q. Peng, M. E. Gibril, X. Wang, S. Wang and F. Kong, *Int. J. Biol. Macromol.*, 2023, **246**, 125668.
- 68 J. Asenbauer, T. Eisenmann, M. Kuenzel, A. Kazzazi, Z. Chen and D. Bresser, *Sustainable Energy Fuels*, 2020, **4**, 5387–5416.
- 69 S. S. Madani, Y. Shabeer, F. Allard, M. Fowler, C. Ziebert, Z. Wang, S. Panchal, H. Chaoui, S. Mekhilef, S. X. Dou, K. See and K. Khalilpour, *Batteries*, 2025, **11**, 127.
- 70 K. Peuvot, O. Hosseinaei, P. Tomani, D. Zenkert and G. Lindbergh, *J. Electrochem. Soc.*, 2019, **166**, A1984.
- 71 Q. Luo, T. Zeng, K. Gu, Q. Lin and W. Yang, *ACS Appl. Energy Mater.*, 2024, **7**, 11610–11632.
- 72 A. K. Padhi, K. S. Nanjundaswamy and J. B. Goodenough, *J. Electrochem. Soc.*, 1997, **144**, 1188.
- 73 S.-Y. Chung, J. T. Bloking and Y.-M. Chiang, *Nat. Mater.*, 2002, **1**, 123–128.
- 74 J. Ye, X. Ji, Z. Liu, K. Liu, J. Li, R. Wang, J. Wang and Q. Lei, *Composites, Part B*, 2024, **277**, 111411.
- 75 A. M. Navarro-Suárez, J. Carretero-González, N. Casado, D. Mecerreyes, T. Rojo and E. Castillo-Martínez, *Sustainable Energy Fuels*, 2018, **2**, 836–842.
- 76 S. V. Gnedenkov, D. P. Opra, S. L. Sinebryukhov, A. K. Tsvetnikov, A. Y. Ustinov and V. I. Sergienko, *J. Solid State Electrochem.*, 2013, **17**, 2611–2621.
- 77 P.-H. Li, Y.-M. Wei, C.-W. Wu, C. Yang, B. Jiang and W.-J. Wu, *RSC Adv.*, 2022, **12**, 19485–19494.
- 78 P. Li, J. Yu, M. Wang, W. Su, C. Yang, B. Jiang and W. Wu, *Int. J. Mol. Sci.*, 2023, **24**, 8661.
- 79 W.-J. Zhang, *J. Power Sources*, 2011, **196**, 13–24.
- 80 S. Wu, R. Xu, M. Lu, R. Ge, J. Iocozzia, C. Han, B. Jiang and Z. Lin, *Adv. Energy Mater.*, 2015, **5**, 1500400.
- 81 L.-L. Yuan, H.-M. Wang, Y.-C. Wu, Q.-X. Hou and R.-C. Sun, *Composites, Part B*, 2024, **287**, 111869.
- 82 J. Domínguez-Robles, M. S. Peresin, T. Tamminen, A. Rodríguez, E. Larrañeta and A.-S. Jääskeläinen, *Int. J. Biol. Macromol.*, 2018, **115**, 1249–1259.
- 83 L. Zhong, Y. Sun, K. Shen, F. Li, H. Liu, L. Sun and D. Xie, *Small*, 2024, **20**, 2407297.
- 84 J.-M. Yuan, W.-F. Ren, K. Wang, T.-T. Su, G.-J. Jiao, C.-Y. Shao, L.-P. Xiao and R.-C. Sun, *ACS Sustainable Chem. Eng.*, 2022, **10**, 166–176.
- 85 H. Lu, A. Cornell, F. Alvarado, M. Behm, S. Leijonmarck, J. Li, P. Tomani and G. Lindbergh, *Materials*, 2016, **9**, 127.
- 86 S. N. Bryntesen, I. Tolstorebrov, A. M. Svensson, P. Shearing, J. J. Lamb and O. S. Burheim, *Mater. Adv.*, 2023, **4**, 523–541.
- 87 S. K. Mohammadian and Y. Zhang, *Int. J. Heat Mass Transfer*, 2018, **118**, 911–918.
- 88 P. Arora and Z. Zhang, *Chem. Rev.*, 2004, **104**, 4419–4462.
- 89 T. Shan, P. Zhang, Z. Wang and X. Zhu, *J. Energy Storage*, 2024, **88**, 111532.
- 90 A. Davoodabadi, C. Jin, D. L. Wood III, T. J. Singler and J. Li, *Extreme Mech. Lett.*, 2020, **40**, 100960.
- 91 W. Hao, X. Bo, J. Xie and T. Xu, *Polymers*, 2022, **14**, 3664.
- 92 C. Liu, Z. Shao, J. Wang, C. Lu and Z. Wang, *RSC Adv.*, 2016, **6**, 97912–97920.
- 93 Y. Li, H. Pu and Y. Wei, *Electrochim. Acta*, 2018, **264**, 140–149.
- 94 M.-J. Uddin, P. K. Alaboina, L. Zhang and S.-J. Cho, *Mater. Sci. Eng. B*, 2017, **223**, 84–90.
- 95 D. Aurbach, Y. Talyosef, B. Markovsky, E. Markevich, E. Zinigrad, L. Asraf, J. S. Gnanaraj and H.-J. Kim, *Electrochim. Acta*, 2004, **50**, 247–254.
- 96 M. Doyle, T. F. Fuller and J. Newman, *Electrochim. Acta*, 1994, **39**, 2073–2081.
- 97 K. Xu, *Chem. Rev.*, 2004, **104**, 4303–4418.
- 98 M. Zhu, J. Wu, Y. Wang, M. Song, L. Long, S. H. Siyal, X. Yang and G. Sui, *J. Energy Chem.*, 2019, **37**, 126–142.
- 99 M. Liu, D. Zhou, Y.-B. He, Y. Fu, X. Qin, C. Miao, H. Du, B. Li, Q.-H. Yang, Z. Lin, T. S. Zhao and F. Kang, *Nano Energy*, 2016, **22**, 278–289.



- 100 X. Zhang, Q. Wu, X. Guan, F. Cao, C. Li and J. Xu, *J. Power Sources*, 2020, **452**, 227833.
- 101 B. Liu, Y. Huang, H. Cao, A. Song, Y. Lin, M. Wang and X. Li, *J. Solid State Electrochem.*, 2018, **22**, 807–816.
- 102 S. Wang, L. Zhang, A. Wang, X. Liu, J. Chen, Z. Wang, Q. Zeng, H. Zhou, X. Jiang and L. Zhang, *ACS Sustainable Chem. Eng.*, 2018, **6**, 14460–14469.
- 103 Z. Liu, T. Karasawa, W. Tan, H. Minegishi, Y. Matsushita, K. Shikinaka, Y. Otsuka and Y. Tominaga, *Polym. J.*, 2024, **56**, 1165–1175.
- 104 H. Y. Jung, J. S. Lee, H. T. Han, J. Jung, K. Eom and J. T. Lee, *Polymers*, 2022, **14**, 673.
- 105 H. Y. Jung, J. S. Lee, H. T. Han, J. Jung, K. Eom and J. T. Lee, *Polymers*, 2022, **14**, 673.
- 106 D. Kai, M. J. Tan, P. L. Chee, Y. K. Chua, Y. L. Yap and X. J. Loh, *Green Chem.*, 2016, **18**, 1175–1200.
- 107 N. Obrzut, R. Hickmott, L. Shure and K. A. Gray, *RSC Sustainability*, 2023, **1**, 2328–2340.
- 108 W.-J. Chen, C.-X. Zhao, B.-Q. Li, T.-Q. Yuan and Q. Zhang, *Green Chem.*, 2022, **24**, 565–584.
- 109 J. Ruwoldt, F. H. Blindheim and G. Chinga-Carrasco, *RSC Adv.*, 2023, **13**, 12529–12553.
- 110 C. Revathy, V. R. Sunitha, B. K. Money, R. Joseph and S. Radhakrishnan, *Ionics*, 2023, **29**, 4025–4035.
- 111 M. Gigli and C. Crestini, *Green Chem.*, 2020, **22**, 4722–4746.
- 112 C. Allegretti, O. Boumezgane, L. Rossato, A. Strini, J. Troquet, S. Turri, G. Griffini and P. D'Arrigo, *Molecules*, 2020, **25**, 2893.
- 113 A.-S. Jääskeläinen, T. Liitiä, A. Mikkelsen and T. Tamminen, *Ind. Crops Prod.*, 2017, **103**, 51–58.
- 114 M. H. Tanis, O. Wallberg, M. Galbe and B. Al-Rudainy, *Molecules*, 2024, **29**, 98.
- 115 T. Pang, G. Wang, H. Sun, W. Sui and C. Si, *Ind. Crops Prod.*, 2021, **165**, 113442.
- 116 C. A. E. Costa, F. M. Casimiro, C. Vega-Aguilar and A. E. Rodrigues, *ChemEngineering*, 2023, **7**, 42.
- 117 J. Xing, S. Bliznakov, L. Bonville, M. Oljaca and R. Maric, *Electrochem. Energy Rev.*, 2022, **5**, 14.
- 118 J. Parameswaranpillai, S. Thomas and Y. Grohens, in *Characterization of Polymer Blends*, John Wiley & Sons, Ltd, 2014, pp. 1–6.
- 119 D. T. Gentekos, R. J. Sifri and B. P. Fors, *Nat. Rev. Mater.*, 2019, **4**, 761–774.
- 120 K. Nikgoftar, A. K. M. R. Reddy, M. V. Reddy and K. Zaghbi, *Batteries*, 2025, **11**, 123.
- 121 W. Li and J. Shi, *Front. Bioeng. Biotechnol.*, 2023, **11**, 1121027.
- 122 I. V. Pylypchuk, A. Riazanova, M. E. Lindström and O. Sevastyanova, *Green Chem.*, 2021, **23**, 3061–3072.
- 123 W. Long, B. Fang, A. Ignaszak, Z. Wu, Y.-J. Wang and D. Wilkinson, *Chem. Soc. Rev.*, 2017, **46**, 7176–7190.
- 124 A. Nebbioso and A. Piccolo, *Anal. Bioanal. Chem.*, 2013, **405**, 109–124.
- 125 B. Apicella, A. Ciajolo, A. Carpentieri, C. Popa and C. Russo, *Fuels*, 2022, **3**, 75–84.
- 126 W. Lin, S. Zhao, B. Lu, F. Jiang, Z. Lu and Z. Xu, *Energy Mater.*, 2024, **4**, 400078.
- 127 P. Molaiyan, G. S. Dos Reis, D. Karuppiah, C. M. Subramaniyam, F. García-Alvarado and U. Lassi, *Batteries*, 2023, **9**, 116.
- 128 J. Liu, X. Mei and F. Peng, *Batteries*, 2022, **8**, 286.
- 129 B. Thomas, M. Sain and K. Oksman, *Nanomaterials*, 2022, **12**, 3630.
- 130 B. Kurc, M. Pięłowska, P. Fuć, N. Szymlet, X. Gross and A. Piasecki, *Ionics*, 2024, **30**, 7431–7451.
- 131 B. Thomas, M. Sain and K. Oksman, *Nanomaterials*, 2022, **12**, 3630.
- 132 A. Beaucamp, M. Muddasar, I. S. Amiin, M. M. Leite, M. Culebras, K. Latha, M. C. Gutiérrez, D. Rodríguez-Padron, F. del Monte, T. Kennedy, K. M. Ryan, R. Luque, M.-M. Titirici and M. N. Collins, *Green Chem.*, 2022, **24**, 8193–8226.
- 133 M. Janssen, E. Gustafsson, L. Echarde and J. Wallinder, Life cycle assessment of lignin-based carbon fibers, 14<sup>th</sup> conference on sustainable development of energy, water and environment systems, Oct 1–6 2019, Ghotenburg, Sweden.
- 134 V. D. Obasa, O. A. Olanrewaju, O. P. Gbenedor, E. F. Ocholor, C. C. Odili, Y. O. Abiodun and S. O. Adeosun, *Atmosphere*, 2022, **13**, 1605.
- 135 A. Beaucamp, M. Muddasar, I. S. Amiin, M. M. Leite, M. Culebras, K. Latha, M. C. Gutiérrez, D. Rodríguez-Padron, F. del Monte, T. Kennedy, K. M. Ryan, R. Luque, M.-M. Titirici and M. N. Collins, *Green Chem.*, 2022, **24**, 8193–8226.
- 136 A. C. Rolandi, I. de Meazza, N. Casado, M. Forsyth, D. Mecerreyes and C. Pozo-Gonzalo, *RSC Sustainability*, 2024, **2**, 2125–2149.
- 137 D. L. Wood, J. D. Quass, J. Li, S. Ahmed, D. Ventola and C. Daniel, *Drying Technol.*, 2018, **36**, 234–244.
- 138 T. Aro and P. Fatehi, *ChemSusChem*, 2017, **10**, 1861–1877.
- 139 A. Kylili, M. Koutinas, P.-Z. Georgali and P. A. Fokaides, *Int. J. Sustainable Energy*, 2023, **42**, 1008–1027.
- 140 J. Zhang, X. Ke, Y. Gu, F. Wang, D. Zheng, K. Shen and C. Yuan, *Int. J. Life Cycle Assess.*, 2022, **27**, 227–237.
- 141 V. D. Obasa, O. A. Olanrewaju, O. P. Gbenedor, E. F. Ocholor, C. C. Odili, Y. O. Abiodun and S. O. Adeosun, *Atmosphere*, 2022, **13**, 1605.
- 142 R. I. Muazu, P. Yaseneva, N. Shah and M.-M. Titirici, *J. Environ. Chem. Eng.*, 2024, **12**, 114387.
- 143 S. Wickerts, R. Arvidsson, A. Nordelöf, M. Swanström and P. Johansson, *J. Ind. Ecol.*, 2024, **28**, 116–129.
- 144 H. Moon, A. Innocenti, H. Liu, H. Zhang, M. Weil, M. Zarrabeitia and S. Passerini, *ChemSusChem*, 2023, **16**, e202201713.
- 145 J. Zhang, H. Xiang, Z. Cao, S. Wang and M. Zhu, *Green Energy Environ.*, 2025, **10**, 322–344.
- 146 S. Srinivasan, S. Shanthakumar and B. Ashok, *Energy Rep.*, 2025, **13**, 789–812.
- 147 D. Pang, H. Wang, Y. Zeng, X. Han and Y. Zheng, *Nanomaterials*, 2025, **15**, 1283.



- 148 S. Paul and P. Shrotriya, *Materials*, 2025, **18**, 613.
- 149 H. Zare-Zardini and R. Ghanipour-Meybodi, in *Handbook of Lignin*, Springer, Singapore, 2025, pp. 741–785.
- 150 L. Yan, A. J. Huertas-Alonso, H. Liu, L. Dai, C. Si and M. H. Sipponen, *Chem. Soc. Rev.*, 2025, **54**, 6634–6651.
- 151 H. Yeo, G. L. Gregory, H. Gao, K. Yiamsawat, G. J. Rees, T. McGuire, M. Pasta, P. G. Bruce and C. K. Williams, *Chem. Sci.*, 2024, **15**, 2371–2379.
- 152 M. Fazeli, S. Mukherjee, H. Baniasadi, R. Abidnejad, M. Mujtaba, J. Lipponen, J. Seppälä and O. J. Rojas, *Green Chem.*, 2024, **26**, 593–630.
- 153 C. G. Yoo and A. J. Ragauskas, in *ACS Symposium Series*, ed. C. G. Yoo and A. Ragauskas, American Chemical Society, Washington, DC, 2021, vol. 1377, pp. 1–12.
- 154 W. Zhang, X. Qiu, C. Wang, L. Zhong, F. Fu, J. Zhu, Z. Zhang, Y. Qin, D. Yang and C. C. Xu, *Carbon Res.*, 2022, **1**, 14.
- 155 M. T. Islam and U. Iyer-Raniga, *Recycling*, 2022, **7**, 33.
- 156 A. Y. Gebreyohannes, S. L. Aristizábal, L. Silva, E. A. Qasem, S. Chisca, L. Upadhyaya, D. Althobaiti, J. A. P. Coutinho and S. P. Nunes, *Green Chem.*, 2023, **25**, 4769–4780.
- 157 L. Coviello, G. Montalbano, A. Piovano, N. Izaguirre, C. Vitale-Brovarone, C. Gerbaldi and S. Fiorilli, *Polymers*, 2025, **17**, 982.
- 158 F. Brienza, D. Cannella, D. Montesdeoca, I. Cybulska and D. P. DeBecker, *RSC Sustainability*, 2024, **2**, 37–90.
- 159 M. Norgren and H. Edlund, *Curr. Opin. Colloid Interface Sci.*, 2014, **19**, 409–416.
- 160 D. Kai, W. Ren, L. Tian, P. L. Chee, Y. Liu, S. Ramakrishna and X. J. Loh, *ACS Sustainable Chem. Eng.*, 2016, **4**, 5268–5276.
- 161 N. A. Alhebshi and H. N. Alshareef, *Mater. Renew. Sustain. Energy*, 2015, **4**, 21.
- 162 I. A. Gilca, V. I. Popa and C. Crestini, *Ultrason. Sonochem.*, 2015, **23**, 369–375.
- 163 Y. Qian, Y. Deng, X. Qiu, H. Li and D. Yang, *Green Chem.*, 2014, **16**, 2156–2163.
- 164 S. Farzin, T. J. Johnson, S. Chatterjee, E. Zamani and S. K. Dishari, *Front. Chem.*, 2020, **8**, 690.
- 165 F. Zhan, S. Liu, Q. He, X. Zhao, H. Wang, M. Han, Y. Yamauchi and L. Chen, *Energy Storage Mater.*, 2022, **52**, 685–735.
- 166 A. Gandini, *Green Chem.*, 2011, **13**, 1061–1083.
- 167 X. Guan, X. Li, X. Zhao, Z. Wang, L. Zhang and J. Ma, *J. Energy Storage*, 2025, **111**, 115380.
- 168 C. Wang, J. Liang, J. Luo, J. Liu, X. Li, F. Zhao, R. Li, H. Huang, S. Zhao, L. Zhang, J. Wang and X. Sun, *Sci. Adv.*, 2021, **7**, eabh1896.
- 169 D. Zheng, J. Zhang, W. Lv, T. Cao, S. Zhang, D. Qiu, Y. Tao, Y. He, F. Kang and Q.-H. Yang, *Chem. Commun.*, 2018, **54**, 4317–4320.
- 170 M. H. Lee, Y. Lee, J. A. Kim, Y. Jeon, M. J. Kim, Y. G. Kim and J. J. Kim, *Electrochim. Acta*, 2022, **419**, 140389.
- 171 J. Maca, M. Frk, Z. Rozsivalova and M. Sedlarikova, *Port. Electrochim. Acta*, 2013, **31**, 321–330.
- 172 T. Bok, S.-J. Cho, S. Choi, K.-H. Choi, H. Park, S.-Y. Lee and S. Park, *RSC Adv.*, 2016, **6**, 6960–6966.
- 173 F. Zhang, Y. Sun, Z. Wang, D. Fu, J. Li, J. Hu, J. Xu and X. Wu, *ACS Appl. Mater. Interfaces*, 2020, **12**, 23774–23780.
- 174 T. Liu, S. Sun, W. Song, X. Sun, Q. Niu, H. Liu, T. Ohsaka and J. Wu, *J. Mater. Chem. A*, 2018, **6**, 23486–23494.
- 175 J. Liu, in *Graphene-based Composites for Electrochemical Energy Storage*, ed. J. Liu, Springer, Singapore, 2017, pp. 51–63.
- 176 Y. Cheng, Z. Chen, H. Wu, M. Zhu and Y. Lu, *Adv. Funct. Mater.*, 2016, **26**, 1487–1487.
- 177 J. Zheng, Y. Wu, C. Guan, D. Wang, Y. Lai, J. Li, F. Yang, S. Li and Z. Zhang, *Carbon Energy*, 2024, **6**, e538.
- 178 L. Mersmann, C. Dias, J. Pires and A. L. Fernando, in *Innovations in Industrial Engineering IV*, ed. J. Machado, J. Trojanowska, K. Antosz, C. P. Leão, L. Knapcikova and A. Sover, Springer Nature Switzerland, Cham, 2025, pp. 192–209.
- 179 M.-S. Lim, G. H. Lim, Y.-J. Shin, J. S. Chae, J.-W. Lee and K. C. Roh, *Energymater*, 2025, **5**, 500104.
- 180 S. Wang, J. Bai, M. T. Innocent, Q. Wang, H. Xiang, J. Tang and M. Zhu, *Green Energy Environ.*, 2022, **7**, 578–605.
- 181 J. P. Jyothibas, R.-H. Wang, Y.-C. Tien, C.-C. Kuo and R.-H. Lee, *Polymers*, 2022, **14**, 3106.
- 182 D. Ji and J. Kim, *Nano-Micro Lett.*, 2024, **16**, 2.
- 183 A. Trezza, L. Mahboob, A. Visibelli, M. Geminiani and A. Santucci, *Appl. Sci.*, 2025, **15**, 8038.

